AD-A125 714 DIAGNOSIS OF FRACTURE DAMAGE IN SIMPLE STRUCTURES: A MODAL METHOD..(U) NEW MEXICO UNIV ALBUQUERQUE BUREAU OF ENGINEERING RESEARCH F D JU ET AL. OCT 82 1/1

UNCLASSIFIED CE-82(82)AFOSR-993-1 AFOSR-TR-83-0049 F/G 5/9 NL

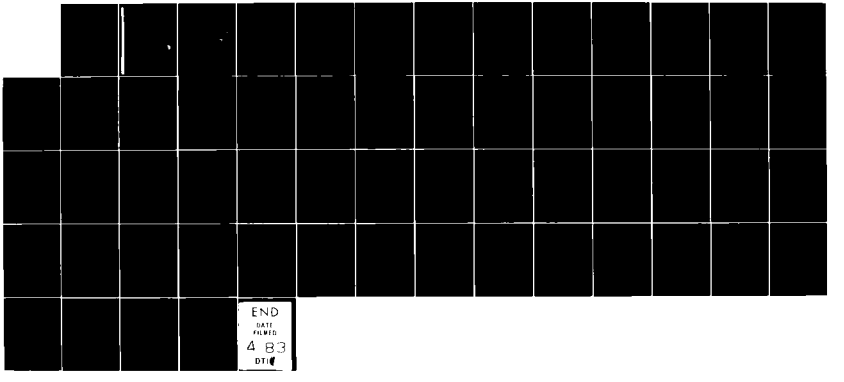

END
DATE FILMED
4 83
DTIC

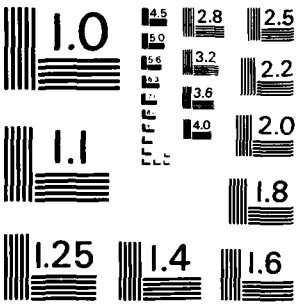

AFOSR-TR- 83-0049

THE UNIVERSITY OF NEW MEXICO
COLLEGE OF ENGINEERING

BUREAU OF ENGINEERING RESEARCH

DIAGNOSIS OF FRACTURE DAMAGE IN SIMPLE STRUCTURES (A MODAL METHOD)

Technical Report

By

Frederick D. Ju
Mehmet Akgün
Thomas L. Paez
Eric T. Wong

Report No. CE-62(82)AFOSR-993-1
Work Performed under AFOSR Contract No. 81-0086

DIAGNOSIS OF FRACTURE DAMAGE IN SIMPLE STRUCTURES (A MODAL METHOD)

by

Frederick D. Ju
Mehmet Akgün
Thomas L. Paez
Eric T. Wong

Submitted to

Air Force Office of Scientific Research

Work Performed under AFOSR Contract No. 81-0086

October 1982

TABLE OF CONTENTS

LIST OF FIGURES

ABSTRACT

The present paper explores a method to locate fracture damage in a structure, and to estimate the intensity of the damage. It is noted that when fracture damage occurs in a structure, the modal frquencies of the damaged structure will shift. The perturbations in individual modal frequencies are governed uniquely by the intensity of the damage and its location in the structure. Consequently, when the frequency spectrum of an unflawed structure is available, field measurement of the structural response after a major event could lead to an estimate of intensity and location of its damage.

The existence of a crack renders an overall softening effect in the compliance of the structure. The reduction in stiffness can be quantified by the location and the intensity of the crack. With such a model, the diagnosis of the fracture damage is fundamentally a structural identification. The effect of fracture at a section may be represented by a spring-loaded hinge of a certain torsional spring coefficient κ. Such representation is based on the criteria of displacement continuity, slope discontinuity at the cracked section and increased compliance. It is demonstrated in the report that the spring coefficient is constant for cross cracks. For one-sided or nonsymmetrical two-sided cracks, the "bilinear spring" may be approximated by a linearized "fracture spring hinge". It is also demonstrated that the spring "constant" is indeed invariant to the location of the fracture. The spring constant is computed by the strain energy release on the crack surface. The shifted modal frequencies are readily the modal frequencies of the same structure with the presence of such a "fracture hinge".

Simple beams, L-frames, and U-frames have been chosen as the basic simple structures. For illustrative purposes, graphs are

constructed in damage-versus-location space, for a specific frequency variation which results from a crack at various locations on the beam with corresponding intensity of damage. A composite of such graphs for several modal frequency variations thus yields the point of specific location and the intensity of the fracture damage. Analytically, the damage function has been programmed to solve for the fracture damage characteristics (γ, e), signifying the intensity of the damage and its location. When there are inadequate measurements of modal frequency variations, the fracture damage characteristics (γ, e) will either be multiple-valued or be some continuous function defined over the structure. Some probability distribution function must be determined or assumed, either from statistics or load distribution or a combination thereof, to give a probability measure to the fracture damage occurrence. A multiple-valued case has been illustrated in the report.

NOMENCLATURE

a	crack length
A	one side of crack surface area
$\{A,B,C\cdots\}$	constant coefficients; specific locations on the structure
b	half depth of a flexural member
e	crack location (= L^*/L)
E	modulus of elasticity
$f(\gamma)$	dimensionless fracture intensity factor
$g(\beta)$	frequency equation
	fracture toughness
$G_k(R_i)$	damage function
I	area moment of inertia
K_I	stress intensity factor for Mode I (open mode) crack
L	characteristic length of a beam
L_i	length of ith members in a structure
ℓ_i	length ratio = L/L_i
$M(x)$	resisting bending moment (at section x) = $EIy''(x)$
n_i	stiffness ratio = $(EI)_i/(EI)$
R_i	relative frequency variations of ith mode = $\Delta\omega_i/\omega_i$
$\underline{U}(P)$	submatrix defined at the location P
ΔU	strain energy increment
$V(x)$	resisting cross-shear (at section x) = $-EIy'''(x)$
x	axial position

$y_i(x)$	modal shape function of ith beam
w	beam width
$w_i(x\ t)$	lateral deflection of ith beam
α_i	characteristic ratio = β_i/β
β	characteristic value $\beta^4 = \omega^2\ pL^4/(EI)$
γ	fracture damage = a/b
κ	torsional spring constant of the fracture hinge
ν	Poisson's ratio
ρ	lineal mass density
θ	sensitivity number
ω_i	ith modal frequency
$\Delta\omega_i$	ith modal frequency shift
ξ_i	dimensionless axial position = x/L

1.0 INTRODUCTION

The problem of fracture diagnosis arises from the need to assure integrity of structures within the means of nondestructive testing. The present report summarizes the modal method to detect and to identify a fracture damage in a simple structure. The simple structures are chosen in the initial effort essentially for their analytical feasibility both in computations and verifications. The very concept shall later be extended to more complex structures and possibly multiple fractures.

It is well known and was studied experimentally and analytically that a structural member loses its load-carrying capacity when a crack is developed in the member [1-3].[1] Structures, which are designed to withstand unusual severe loadings such as earthquakes to buildings, sudden pressurization in reactor vessels, or blast loads to aerospace structures, may develop cracks either through aging or as a result of an event of excitation. The damaged structure, if not detected and corrected, may not be able to withstand the severe loadings according to design. ASME Code [4] has identified crack inspection methods by visual, surface, and volumetric methods. The cracks may escape the visual and surface examinations because of sheltering by coating or other structural components, or simply due to oversight. Radiographic volumetric method has been successfully employed for some structures. It is however limited by its expense, by the range limitation, and by the complexity of the structure. In searching for other means, it is proposed in the present report that fracture, in general, changes the dynamic characteristics of the structure. Furthermore, for small oscillations, the dynamic parameters are assumed to be delineative in the damping and the stiffness properties. This report shall study only the change in the stiffness parameter, and its relationship to fracture characteristics of the structure. The change is in turn to be measured by the change in modal frequencies.

[1] Numbers in brackets denote the references.

Recently, Chondros and Dimarogonas [5] experimentally determined the change of modal frequencies of a cantilever beam, which was caused by crack at the welded built-in end. The changes in frequencies are related analytically then to those of a cantilever beam which is supported by a spring-loaded hinge at the built-in end. In the present report, the basic concept will be expanded further to establish a theoretical base of fracture diagnosis by measurement of frequency variations. The method will then be demonstrated applicable to other configurations of simple structures with the crack at any possible location.

2.0 THEORY

2.1 Damage Function

The fractured structure is to be characterized by the fracture intensity (γ) and the location (e). The fracture intensity is essentially defined through the geometry of the crack. If there are N cracks, the fracture damage of the structure is hence defined by a set of $\{\gamma_k, e_k\}$, k = 1,2,...,N. Because of the presence of the N cracks, the modal frequencies $\{\omega_i\}$ will be changed, usually reduced, by the amount $\{\Delta\omega_i\}$. The set of relative frequency variations $\{R_i\}$ is defined as

$$R_i = \Delta\omega_i / \omega_i . \tag{1}$$

The relative frequency variation can be functionally expressed as

$$R_i = f_i(\gamma_k, e_k \; ; \text{ structural parameters}), \tag{2}$$

when it is assumed that the frequency variations can be measured immediately before and after the damage-causing event. The structural parameters may be considered as constants. A simplified form of Equation (2) is hence

$$R_i = f_i(\gamma_k, e_k). \tag{3}$$

If we exclude the case of repeated modal frequencies, the inverse of Equation (3)[2] exists as

$$(\gamma, e)_k = G_k(R_i), \tag{4}$$

where every G_k represents a pair of functions for the pair of fracture characteristics $(\gamma, e)_k$.

Numbers in parentheses refer to equations.

With known and sufficient measurements of the frequency variations, R_i, the damage characteristics can be determined with given functional expressions $\{G_k(R_i)\}$, which are therefore referred to as the damage functions. The damage functions can be established experimentally, as done by Chondros and Dimarogonas [5] for a fixed location e = 0. They may also be determined analytically; the present report addresses this problem in the sequel. Theoretically, given adequate measurements of the frequency variations the fracture damage $(\gamma, e)_k$ can be determined uniquely. But uncertainty rises through many factors, such as the number of measurable modal frequencies, the possible cross-over of frequency-shifts. Even the damage functions themselves may be probabilistic. As a general illustration, let there be inadequate M measurements of frequency variations for a known number, N, of cracks, such that $M < 2N + 1$. The damage function (4) will not be sufficient to solve for the fracture characteristics (γ, e) deterministically. In that case, a probability density function $p(\gamma, e)$ is to be established to identify the probability of fractures at certain locations, such that

$$p(\gamma, e) = p(\gamma/e)\, p(e). \tag{5}$$

As an example, when N = 1 and M = 2, the solutions to fracture characteristics form a discrete set of K pairs such that $K > 1$. The probability distribution function of the pairs in the solution set is then given by:

$$F(\gamma, e) = \sum_{k=1}^{K} p_j H[(\gamma, e) - G_j(R_i)],\ i = 1, 2 \tag{6}$$

where $H(x)$ is the Heaviside function that $H(x) = \begin{cases} 1 & x \geq 0 \\ 0 & x < 0, \end{cases}$ p_j is the probability that the solution equals the jth pair $(\gamma, e)_j$ in the solution set and

$$\sum_{j=1}^{K} p_j = 1 \tag{7}$$

When N = 1 and M = 1 there will be infinitely many possible solution pairs to the equation (4), in which case $F(\gamma, e)$ will be a continuous function.

2.2 Fracture Hinge

As a point of departure, we shall consider a fracture geometry shown in Figure 1a. Under flexural loading, the crack (a) is the Mode I (open-mode) crack. The intensity of the fracture damage in such a geometry is defined by $\gamma = a/b$ at the position $e = L^*/L$. The existence of a crack in a structural member renders an overall softening effect in the compliance of the structure. The reduction in stiffness can be quantified by the location and the geometry of the crack. For bar structures, the lower frequency modes are generally flexural. A crack in a flexural member suggests a slope-discontinuity at the section containing the crack, although the displacement is still continuous there. The effect of fracture at a section may therefore be represented by a spring-loaded hinge of a torsional spring coefficient, κ, which may be determined either analytically or experimentally [5], Figure 1b. The principal concerns are whether the *spring coefficient is a constant* (i.e., load/displacement-independent) and is invariant to the location along the flexural member. In other words, for analytical feasibility, the "fracture hinge" should be entirely characterized by the intensity of the fracture damage which is $\gamma = a/b$ in the present case.

Development of the simulation is to be based on the equivalence of energy contents of flexural members, one with a cracked section, another with a hinge. If the "fracture hinge" in the simulated beam is linear, the energy stored in the torsional spring is

$$\Delta U = \frac{1}{2}\frac{M^2}{\kappa}, \tag{8}$$

where M is the resisting moment at the location of the fracture hinge. It is observed that when there is no crack the spring constant approaches infinity. The softening effect of the crack

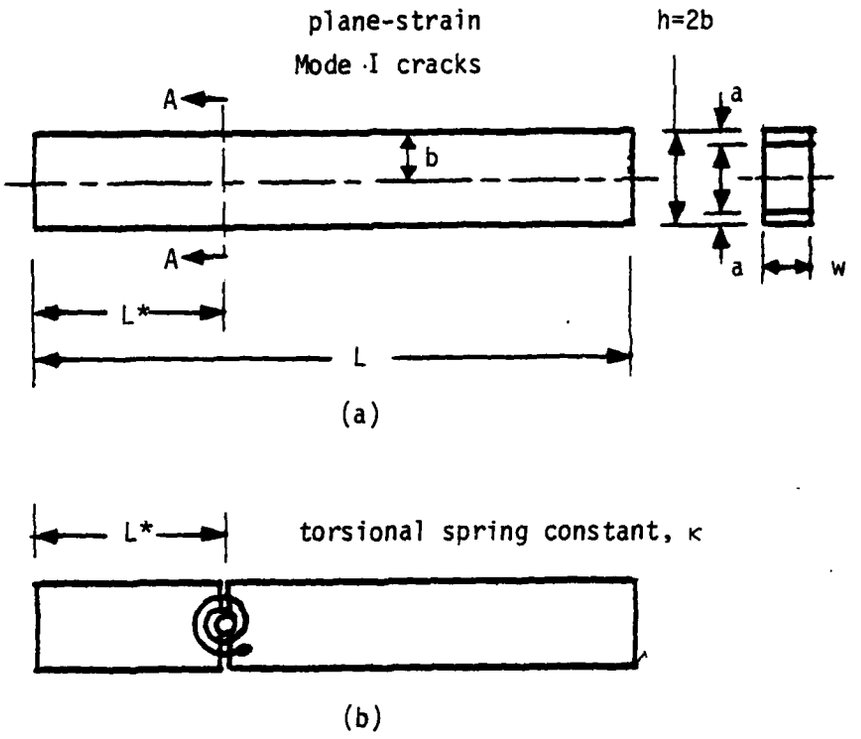

Figure 1. Fracture geometry and equivalent fracture hinge.

results in an increase of energy content under load-prescribed condition [6]. The increase in energy is provided by the surface energy of the crack. Hence, assuming that the crack geometry is stable for Mode I crack,

$$\Delta U = \int_0^A G dA = \frac{1 - \nu^2}{E} \int_0^A K_I^2 \, dA \tag{9}$$

where G is the fracture toughness, A is the area of one side of the crack surface, K_I is the stress intensity factor for Mode I crack. The stress intensity factor is related to the loading and geometry as

$$K_I = \sigma_0 \sqrt{\pi a} \, f(\gamma) = \frac{M}{Z} \sqrt{\pi a} \, f(\frac{a}{b}) \tag{10}$$

where a is the crack depth, b is the half depth of the beam, M is the resisting moment at the cracked sction, Z is the section modulus and $f(\gamma)$ is the dimensionless fracture intensity factor. For a beam of rectangular cross-section, $f(\gamma)$ can be obtained from expressions given by Bentham and Koiter [7] as

$$f(\gamma) = (1 - \gamma)^{-1.5} [1.122 - 2.363\gamma + 4.367\gamma^2 - 4.88 \gamma^3 + 2.845 \gamma^4 - 0.663 \gamma^5]. \tag{11}$$

Combining equations (8, 9, 10) we thus arrive at the spring constant

$$\kappa = \frac{EZ^2}{2(1 - \nu^2)\pi} \Big/ \int_0^A a[f(\gamma)]^2 dA. \tag{12}$$

For a rectangular cross section, $Z = 2/3 \, b^2 w$, where w is the width. Therefore

$$\kappa = \frac{2Eb^2w}{9(1-\nu^2)\pi} \Big/ \int_0^{\gamma} \lambda[f(\lambda)]^2 d\lambda \tag{13}$$

or in its dimensionless form (shown in Figures 2a, b, c)

$$\bar{\kappa} = \frac{(1-\nu^2)\kappa}{Eb^2w} = \frac{2}{9\pi} \Big/ \int_0^{\gamma} \lambda[f\lambda)]^2 d\lambda \tag{13a}$$

The expression in (13) therefore shows that the torsional spring coefficient is entirely determined by the crack geometry for a locally uniform beam of a specific material. The equivalent "fracture hinge" indeed has a linear torsional spring.

It is noted that Figure 1a illustrates a beam with symmetrical cracks. During flexural vibration, the tension side will open to provide the softening effect. The compression side is closed, thus contributes nothing toward the hinge effect. The fracture hinge, therefore, has a linear torsional spring provided that the cracks on two sides are symmetrical. Asymmetry leads to bilinear springs. In that case the torsional spring will be approximated by a linear spring with equivalent period. As an illustration, we shall consider the extreme case of a one-sided crack. In such case, the frequency of the beam is the same as that of an uncracked one when the crack is closed; the frequency will be that of a symmetrically cracked one when the crack is open. Let $\tau_1/2$ be the half-period of modal oscillation when the cracked side is in compression and $\tau_2/2$ be the half-period when the cracked side is in tension. Figure 3 shows the one complete period of a one-side cracked beam. The period of the beam with one-side crack is therefore

$$\tau = \frac{1}{2}(\tau_1 + \tau_2).$$

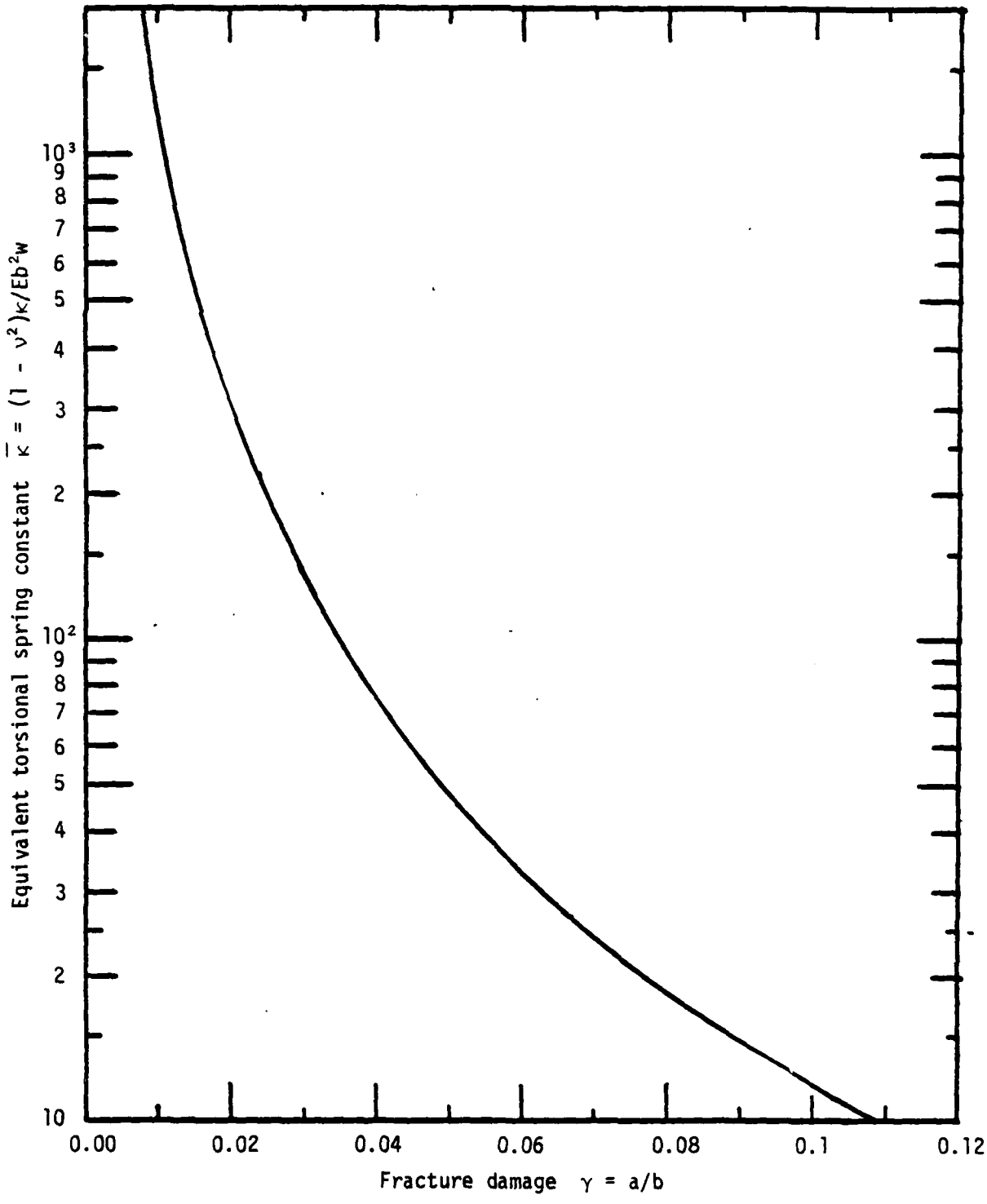

Figure 2a. Spring constant for shallow crack.

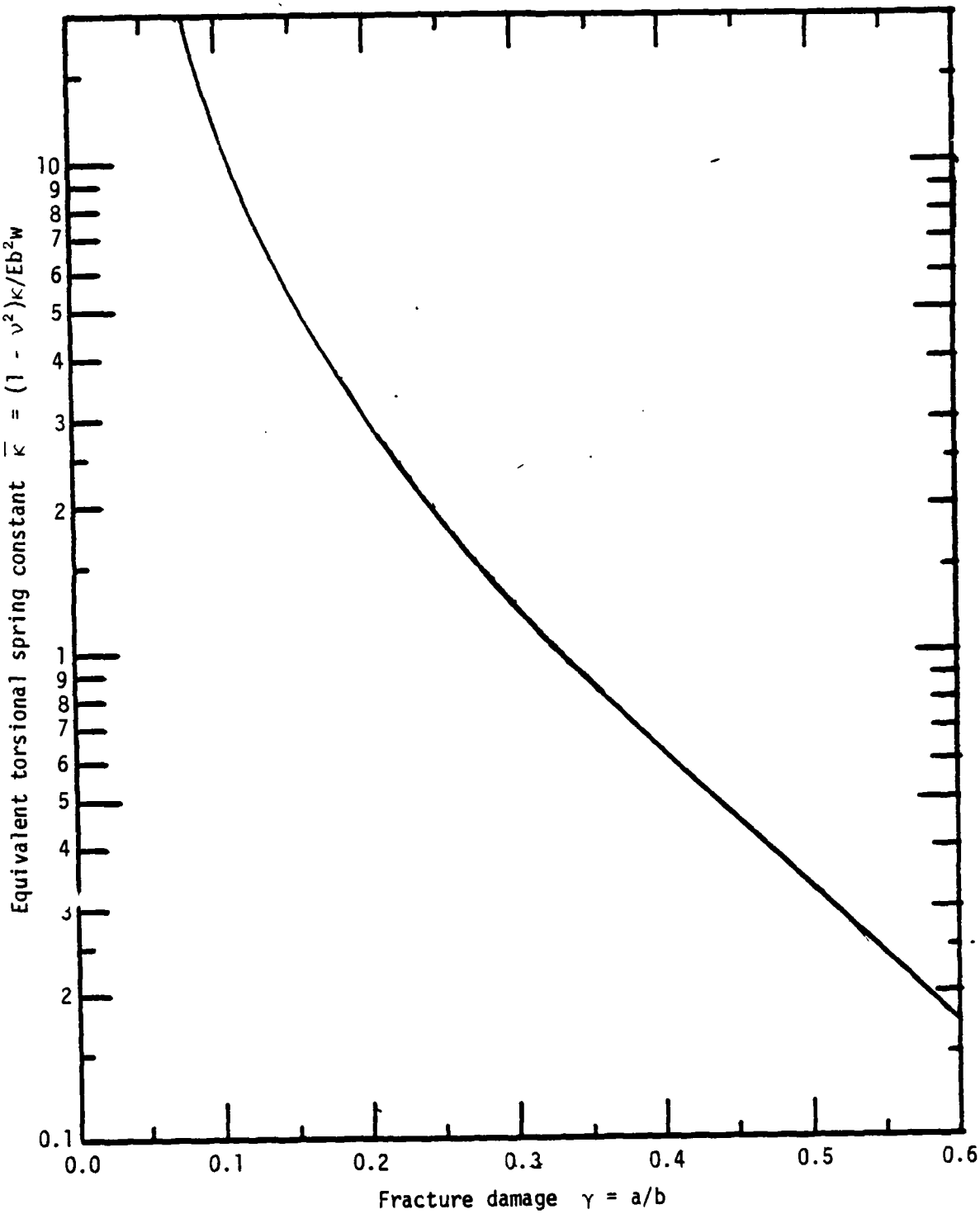

Figure 2b. Spring constant for deeper crack

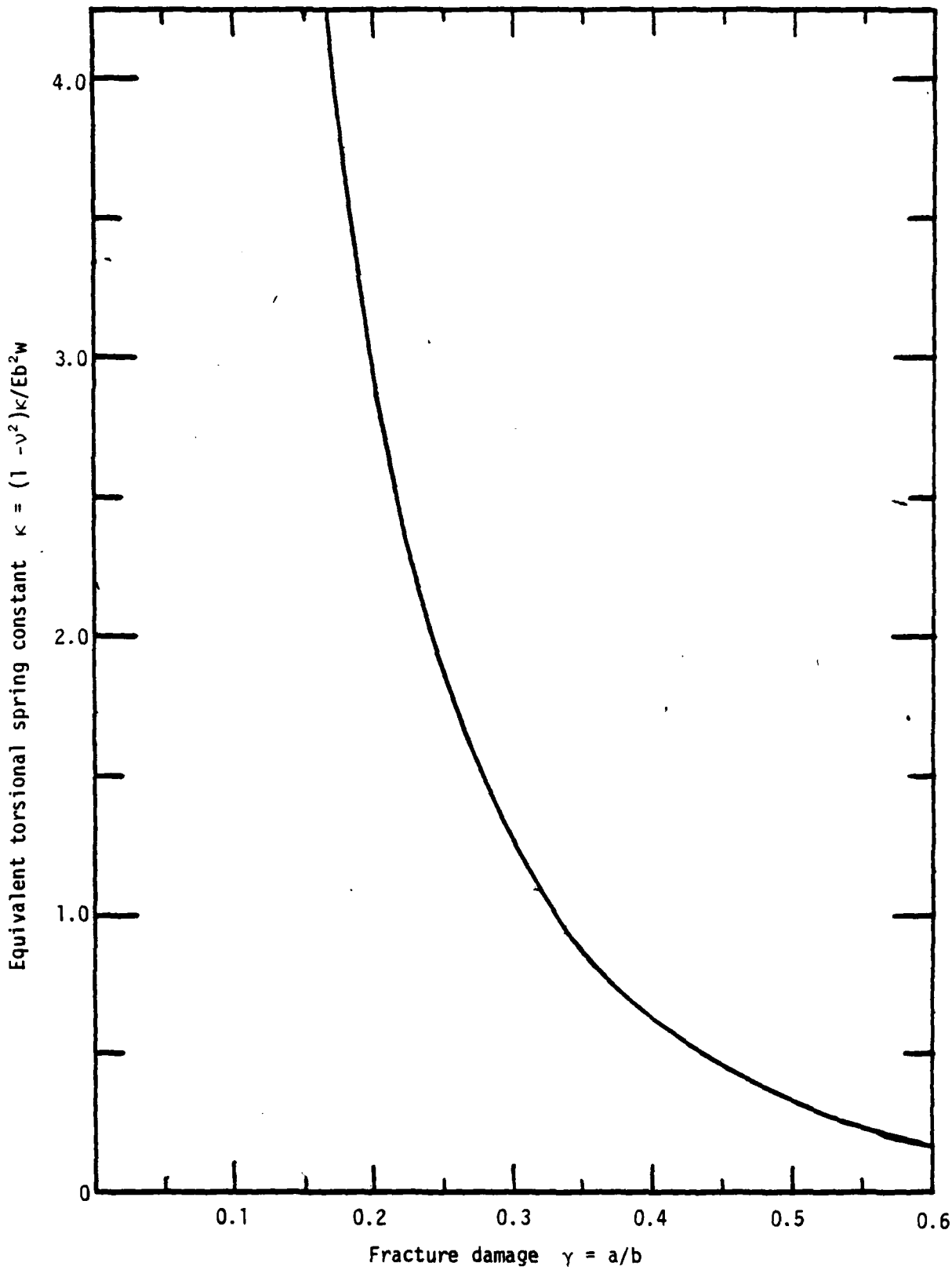

Figure 2c. Spring constant for deeper crack.

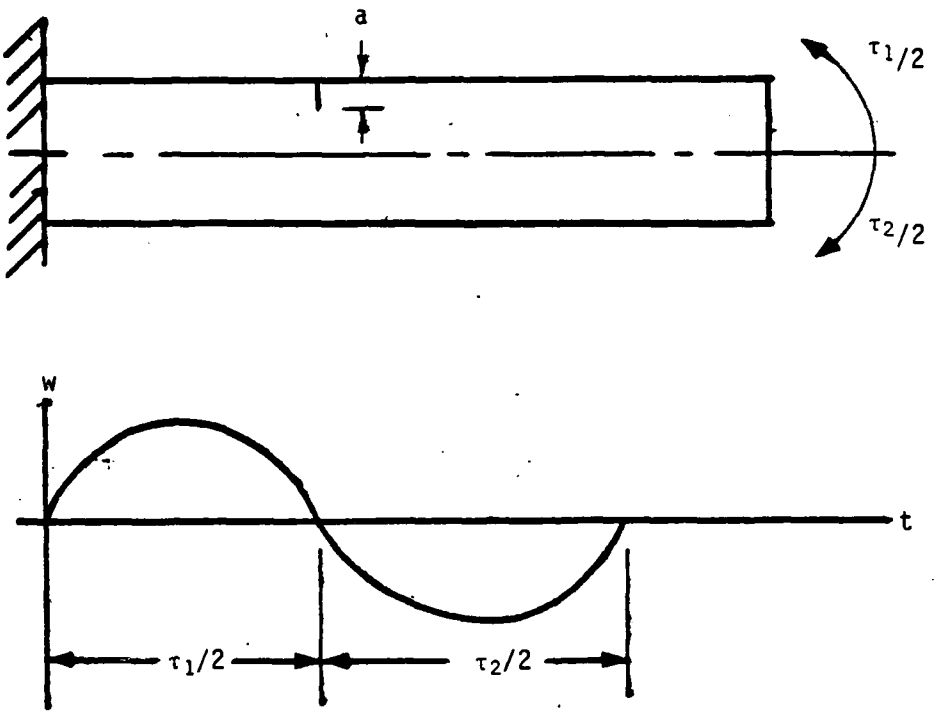

Figure 3. Period of a one-sided crack.

When we designate ω_1 the modal frquency of the uncracked beam, $\Delta\omega_1$ its change for beam with symmetrical cracks, and $\Delta\omega$ the frequency change of the one-side cracked beam, we have then $\tau_1 = 2\pi/\omega_1$, $\tau_2 = 2\pi/(\omega_1 - \Delta\omega_1)$ and $\tau = 2\pi/(\omega_1 - \Delta\omega)$, or

$$\frac{1}{\omega_1 - \Delta\omega} = \frac{1}{2}\left(\frac{1}{\omega_1} + \frac{1}{\omega_1 - \Delta\omega_1}\right).$$

Frequency variation $\overline{R}$ is therefore

$$\overline{R} = \frac{\Delta\omega}{\omega_1} = \frac{R}{(2 - R)} \quad \text{or} \quad R = \frac{2\overline{R}}{(1 + \overline{R})}$$

where R is the frequency variation of beam with symmetrical cracks for the same depth of crack. Figure 4 shows the relationship of the frequency variations. The probability of asymmetry at the cracked section accounts for the random characteristics of the function in (4). In the present report, the fracture diagnosis will be limited to that of symmetrical cracks only. The pair of fracture damage characteristics are then $\gamma = a/b$ and $e = L^*/L$.

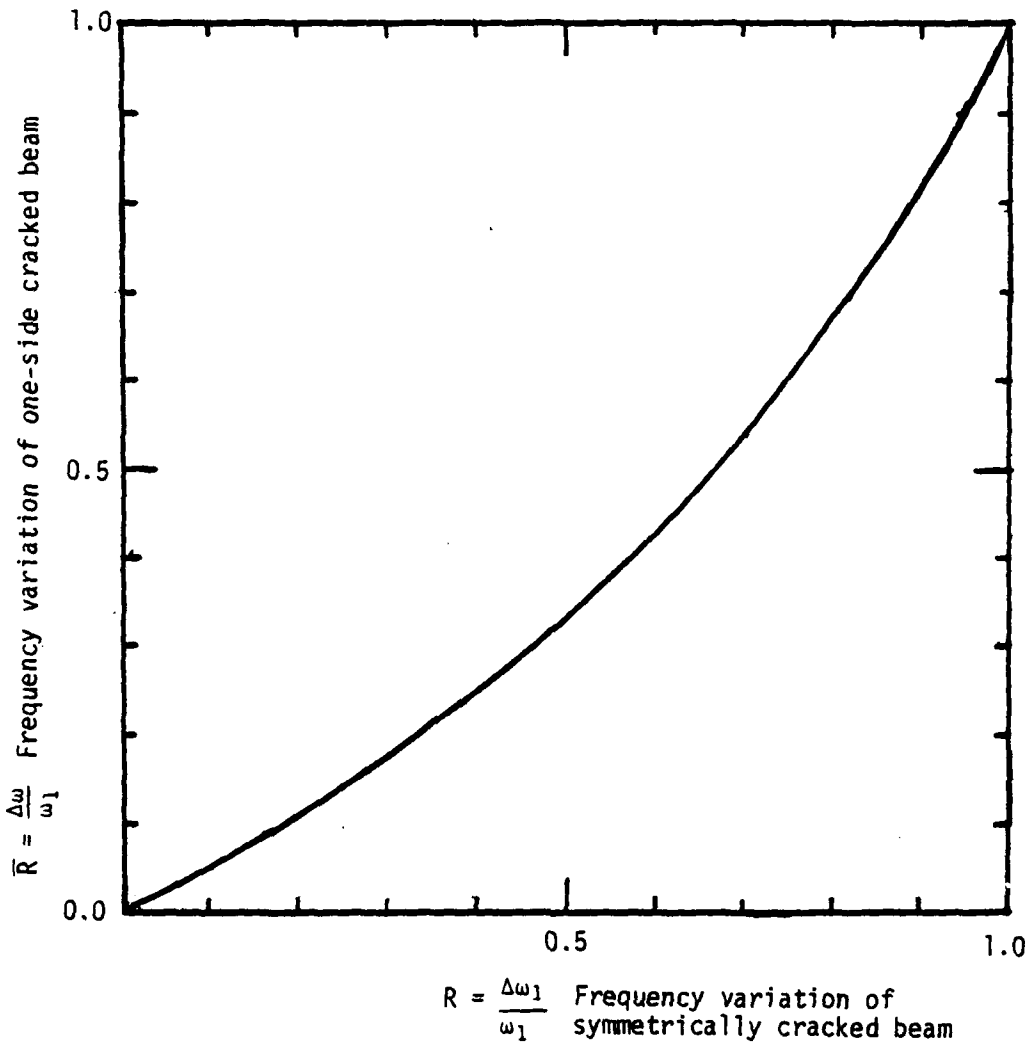

Figure 4. Frequency variations.

2.3 Fracture Diagnosis

In order to identify the damage on the structure, it is important to have a priori a definitive effect of the damage on the structure; that is, it is necessary to establish the damage function (4), analytically or experimentally. For structures composed of flexural members, the deformation of the entire structure can be defined by a lateral displacement set $\{w_i(x_i,t)\}$, governed by a set of differential equations

$$(EI)_i \frac{\partial^4 w_i}{\partial x_i^4} + \rho_i \frac{\partial^2 w_i}{\partial t^2} = 0 \qquad (15)$$

where $(EI)_i$ is the beam stiffness and ρ_i is the lineal mass density of the ith section of the structure; summation convention is not applied in the equation. At the modal oscillation of frequency ω, the displacement is defined by the modal shapes $\{y_i(x_i)\}$

$$w_i(x_i, t) = y_i(x_i) \sin \omega t.$$

The set of differential equations (15) become the modal shape equations;

$$y_i'''' - \frac{\omega^2 \rho_i}{(EI)_i} = 0$$

where the primes (') indicate derivatives with respect to the argument x_i. In terms of dimensionless variables

$\xi_i = x_i/L_i$, $\beta_i^4 = \omega^2 \rho_i L_i^4/(EI)_i$, the modal shape equations become

$$y_i'''' - \beta_i^4 y_i = 0. \qquad (16)$$

Let there be a reference section (ρ, EI, L); the characteristics of all other sections can be defined as

$$\alpha_i^4 = (\beta_i/\beta)^4 = \frac{\rho_i}{\rho}\frac{EI}{(EI)_i}\left(\frac{L_i}{L}\right)^4 \tag{17}$$

$n_i = (EI)_i/(EI)$ and $\ell_i = L/L_i$. The general solutions are:

$$y_i(\xi_i) = A_i\cosh(\alpha_i\beta\xi_i) + B_i\sinh(\alpha_i\beta\xi_i) + C_i\cos(\alpha_i\beta\xi_i) + D_i\sin(\alpha_i\beta\xi_i). \tag{18}$$

With application of boundary conditions, a characteristic equation can be established

$$g_1(\beta) = 0. \tag{19}$$

From the set of characteristic values $\{\beta\}$ the modal frequencies $\{\omega\}$ can be determined as

$$\omega = \frac{\beta^2}{L^2}\sqrt{\frac{EI}{\rho}}. \tag{20}$$

When a crack is developed at a location L*, as shown in Figure 1a, the member is to be divided into two separate flexural members with modal shapes $\{y_1, y_2\}$ that satisfy certain continuity conditions at the crack location. The conditions are

$$y_1(L^*) = y_2(L^*),\ y_1''(L^*) = y_2''(L^*),\ y_1'''(L^*) = y_2'''(L^*)$$

and

$$\kappa[y_2'(L^*) - y_1'(L^*)] = EIy_1''(L^*).$$

The first three conditions are displacement and forces continuity, the last condition is the spring hinge effect. In terms of dimensionless quantities, $e = L^*/L$ and $\theta = EI/\kappa L$, the conditions become

$$\left.\begin{aligned} &y_1(e) = y_2(e), \quad y_1''(e) = y_2''(e), \quad y_1'''(e) = y_2'''(e) \\ &\text{and} \\ &\theta y_1''(e) = y_2'(e) - y_1'(e) \end{aligned}\right\} \tag{21}$$

The weakened structure will result in another characteristic equation

$$g_2(\bar{\beta};\ \theta,\ e) = 0. \tag{22}$$

where θ and e are the governing parameters for the solution set of new characteristic values, $[\bar{\beta}(\theta, e)]$. The new frequency set is similar to (20) as

$$\bar{\omega}(\theta,e) = \omega - \Delta\omega(\theta,e) = \frac{\bar{\beta}^2}{L^2}\sqrt{\frac{EI}{\rho}}. \tag{20a}$$

From the expressions in (20) and (20a), the damage functions (4) are determined. The pair of governing parameters are θ and e, rather than γ and e. For a rectangular cross section, θ has the value,

$$\theta = 3\pi(1 - \nu^2)\left(\frac{b}{L}\right)\int_0^{\gamma}\lambda[f(\lambda)]^2 d\lambda \tag{23}$$

The parameter θ is seen to be principally affected by the fracture damage (γ) and the slenderness ratio (b/L). The measurements of frequency variations $\{R_i\}$ are related to fracture damage through this dimensionless parameter, hence called the sensitivity number; that is, the greater the value of the sensitivity number, the larger are the variations in modal frequencies. Its value, in $\theta/(1 - \nu^2)$, is graphed in Figure 5.

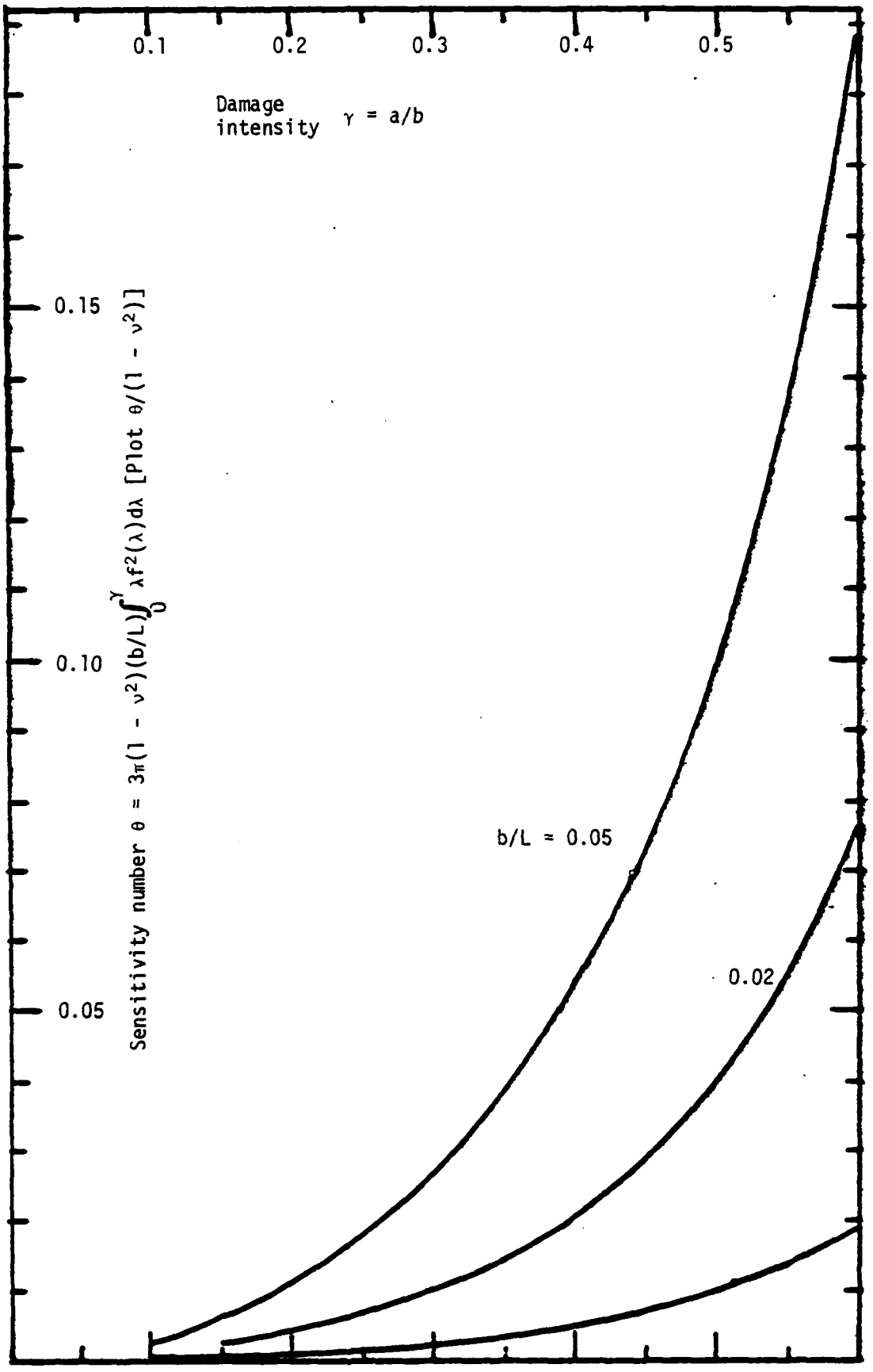

Figure 5. Sensitivity number versus damage intensity.

3.0 DAMAGE DIAGNOSIS IN SIMPLE STRUCTURES

The principle of damage diagnosis is to be applied and illustrated to some simple structures; namely a simple beam, an L-frame, and a U-frame, Figure 6.

3.1 Simple Beam

The modal frequencies for a simple beam can be readily established analytically. Those of an uncracked beam are available from many standard publications, such as Young and Felgar [8]. The solution of the shape function $y(\xi)$ is

$$y(\xi) = A \cosh(\beta\xi) + B \sinh(\beta\xi) + C \cos(\beta\xi) + D \sin(\beta\xi) \quad (24)$$

Two homogeneous kinematic forced boundary conditions or two kinetic natural boundary conditions or mixed two are available at each end ($\xi = 0$ or 1). For the resulting set of homogeneous equations, the determinant of coefficients for {A B C D} must be zero for non-trivial solutions. The characteristic equation in β (19) is

$$g_1(B) = \begin{vmatrix} \underset{\sim}{U}_1(A) \\ \\ \underset{\sim}{U}_6(B) \end{vmatrix} = 0, \quad (19a)$$

where $\underset{\sim}{U}_1(A)$ and $\underset{\sim}{U}_6(B)$ are two (2 x 4) matrices corresponding to the boundary conditions at A and B, i.e., $\xi = 0$ and 1, respectively. For instance, for the cantilever end conditions

$$\underset{\sim}{U}_1(A) = \begin{bmatrix} 1 & 0 & 1 & 0 \\ 0 & 1 & 0 & 1 \end{bmatrix} \quad (25)$$

$$\underset{\sim}{U}_6(B) = \begin{bmatrix} \cosh\beta & \sinh\beta & -\cos\beta & -\sin\beta \\ \sinh\beta & \cosh\beta & \sin\beta & -\cos\beta \end{bmatrix} . \quad (26)$$

1. Simple beam

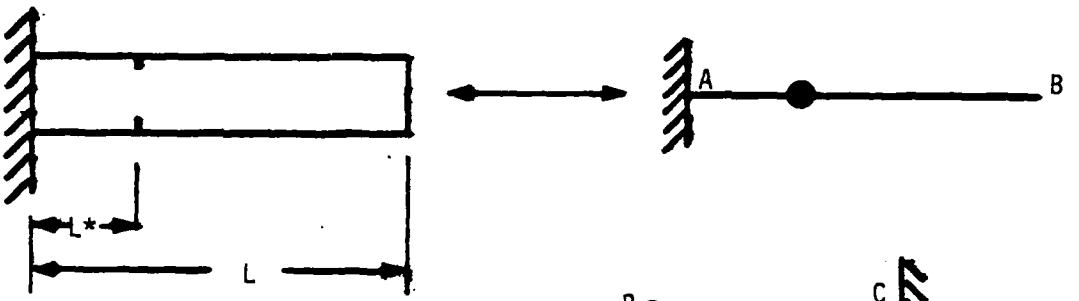

2. L-Frame

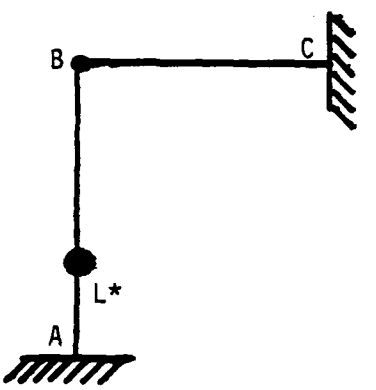

3. U-Frame

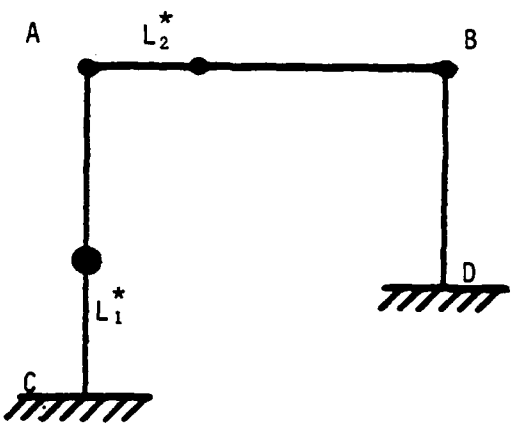

Figure 6. Simple structures with fracture damage.

The solution set $\{\beta_i\}$ thus leads to the modal frequencies $\{\omega_i\}$ of an uncracked beam by (20).

$$\omega_i = \left(\frac{\beta_i}{L}\right)^2 \sqrt{\frac{EI}{\rho}}.$$

For a beam with a crack at the section L*, Figure 1a, the modal shape function is divided into two parts, $y_1(\xi)$ and $y_2(\xi)$, for the range (0, e) and (e, 1), respectively, where e = L*/L. Each portion of the shape function must satisfy the governing equation (16) and have a general expression as (18). The additional continuity conditions (21) expand the order of determinant of the characteristic equation by four, to result in

$$g_2(\bar{\beta}) = \begin{vmatrix} \underset{\sim}{U}_1(A) & \underset{\sim}{0} \\ \underset{\sim}{U}_3(e) & \underset{\sim}{U}_4(0) \\ \underset{\sim}{0} & \underset{\sim}{U}_6(B) \end{vmatrix} = 0 \qquad (27a)$$

where both null matrices $\underset{\sim}{0}$ are (2 x 4), $\underset{\sim}{U}_3(e)$ and $\underset{\sim}{U}_4(e)$ are both (4 x 4) with expressions:

$$\underset{\sim}{U}_3(\beta,e,I) = \begin{bmatrix} 0 & 0 & 0 & 0 \\ 0 & 0 & 0 & 0 \\ 0 & 0 & 0 & 0 \\ \theta\bar{\beta}\cosh(\bar{\beta}e) & \theta\bar{\beta}\sinh(\bar{\beta}e) & -\theta\bar{\beta}\cos(\bar{\beta}e) & -\theta\bar{\beta}\sin(\bar{\beta}e) \end{bmatrix}$$

$$- \underset{\sim}{U}_4(\bar{\beta},e) \qquad (27)$$

$$U_4(\beta,e) = \begin{bmatrix} \cosh(\bar{\beta}e) & \sinh(\bar{\beta}e) & \cos(\bar{\beta}e) & \sin(\bar{\beta}e) \\ \cosh(\bar{\beta}e) & \sinh(\bar{\beta}e) & -\cos(\bar{\beta}e) & -\sin(\bar{\beta}e) \\ \sinh(\bar{\beta}e) & \cosh(\bar{\beta}e) & \sin(\bar{\beta}e) & -\cos(\bar{\beta}e) \\ \sin(\bar{\beta}e) & \cosh(\bar{\beta}e) & -\sin(\bar{\beta}e) & \cos(\bar{\beta}e) \end{bmatrix} \quad (28)$$

The frequency variations $\{R_i\}$ can be computed as functions of (θ, e), subsequently $(\gamma, e; b/L)$, where the slenderness ratio b/L is an influencing parameter. Figure 7 (a, b, c) show three modal frequency variations for a cantilever beam of a slenderness ratio of $b/L = 0.05$, representing the function f_i in (3). Figure 8 shows the corresponding inverse transform for the damage function G_k in (4), with specific given frequency variations: $R_1 = 0.02$, $R_2 = 0.01$, and $R_3 = 0.0225$. For a beam with a single crack, the two unknowns (γ, e) should be solvable with two frequency variations (say R_1, R_2). However, as it is observed in Figure 8 for the range of e: [0, 1], there are two solution points: $e_1 = 0.08$ and $e_2 = 0.33$, the intersections of R_1 and R_2 curves. Yet, the solution must also satisfy the other frequency variations as well; in the present case, the third mode. The only solution is therefore at $e = 0.33$ corresponding to a crack damage intensity of 0.32. Figure 9 shows the damage function (4) for given modal frequency variations: $R_1 = 0.026$, $R_2 = 0.096$, and $R_3 = 7.33 \times 10^{-5}$. The resulting fracture characteristic pair is $(\gamma, e) = (0.6, 0.5)$.

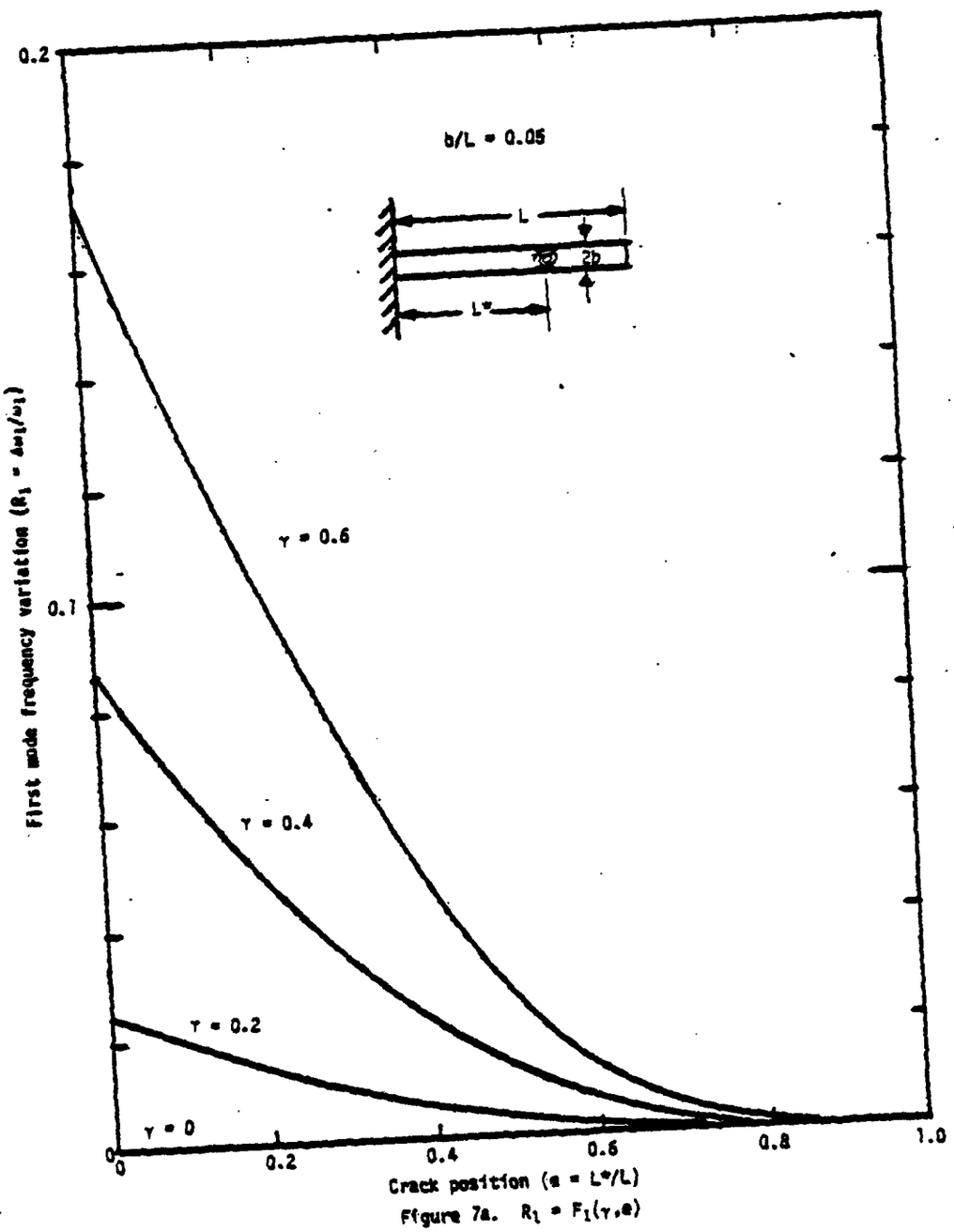

Figure 7a. $R_1 = F_1(\gamma, \alpha)$

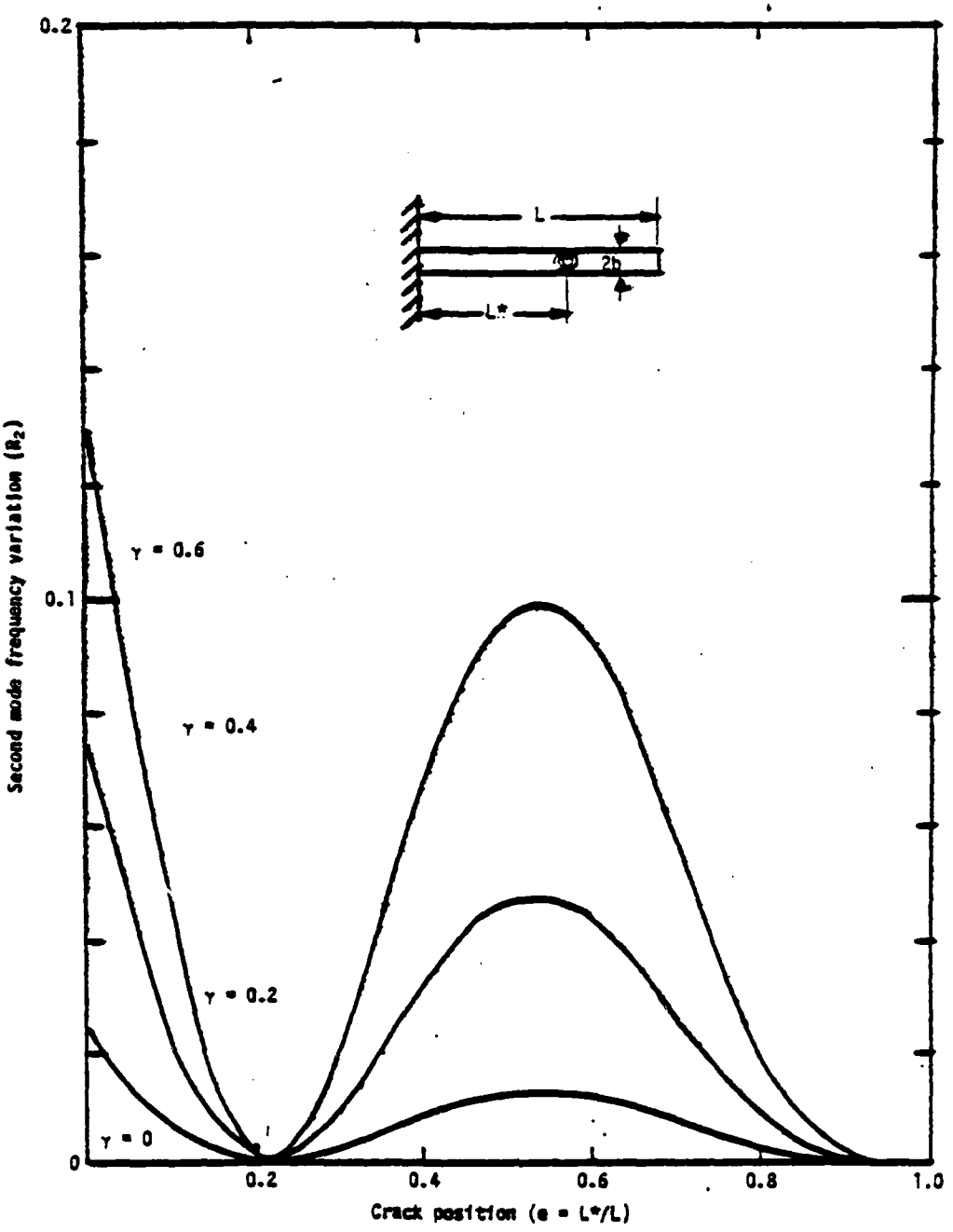

Figure 7b. $R_2 = F_2(\gamma,\alpha)$

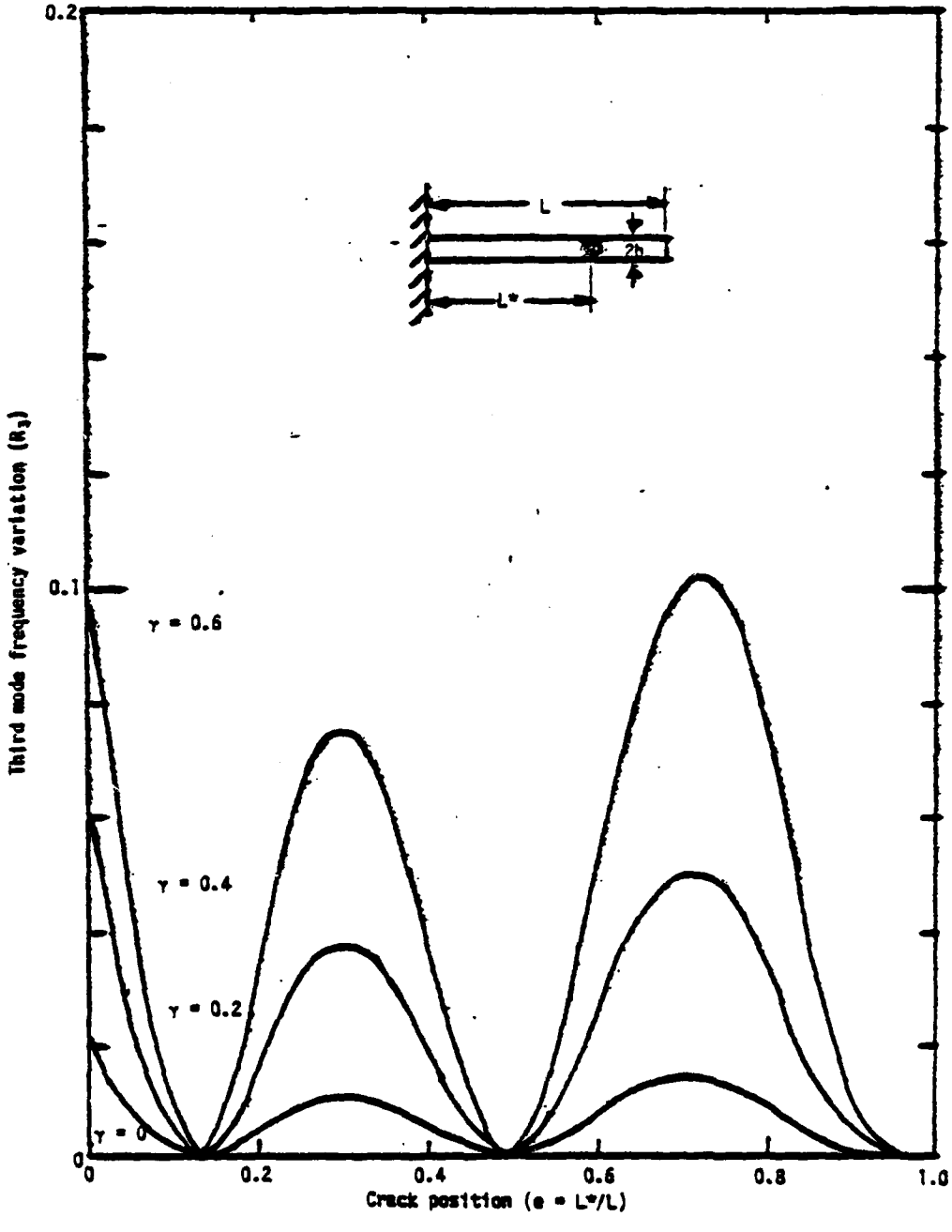

Figure 7c. $R_3 = F_3(\gamma, e)$

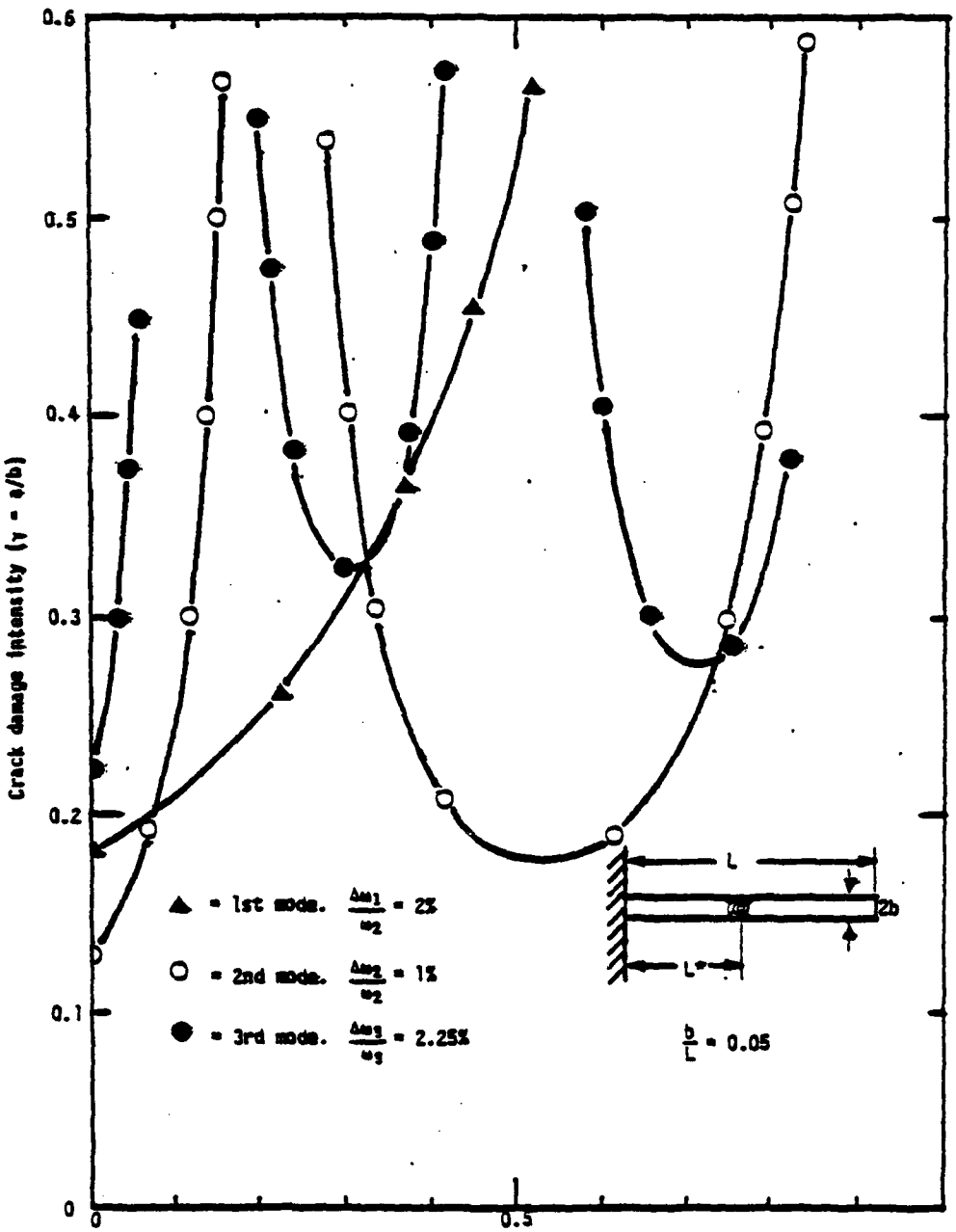

Figure 8. $(\gamma, e) = G(R_1)$

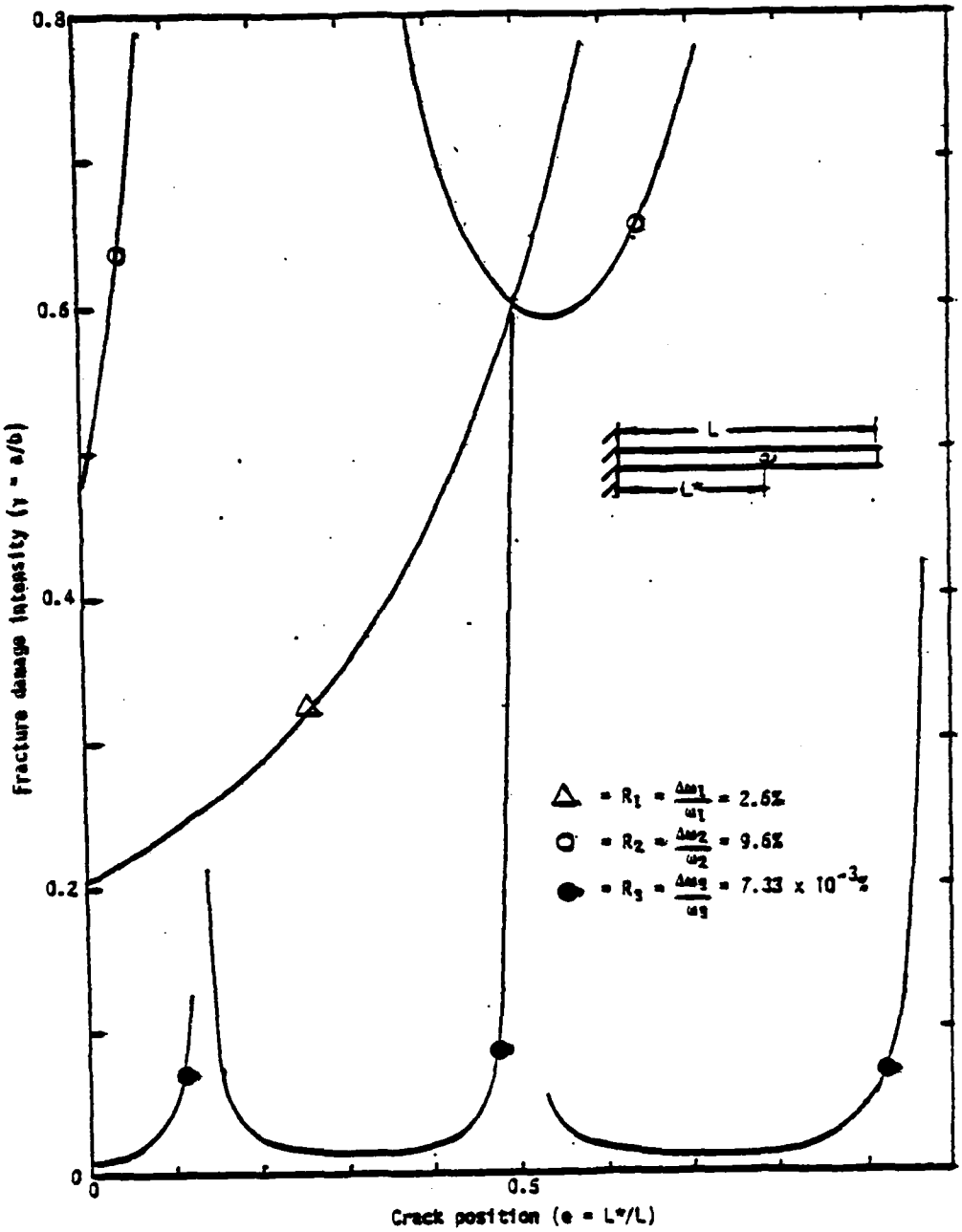

Figure 9. Damage function $(\gamma, e) = G(R_i)$

3.2 L-Frame

The modal frequency analysis of a simple L-frame is usually carried out as two beams rigidly connected at the corner. The contraction in axial length is treated as second-order smallness in comparison to the lateral displacement. In the case when both anchors are either fixed or pinned, the displacement at the junction corner is therefore approximated by order magnitude to be zero. If one of the anchors is allowed to displace axially, the inertial effect of the beam containing the free terminus must be accounted for by Newton's second law. Since the free terminus condition will be demonstrated in the U-frame problem, we shall, for illustrative purpose of the damage diagnosis, choose as an example an L-frame with both termini fixed. Without loss of generality, the cracked section is placed on the vertical leg, Figure 10. The continuity conditions and geometrical constraints at the corner with reference to the general solution (18) are:

$$y_1(1) = 0, \quad y_2(0) = 0, \quad \ell_1 y_1'(1) = \ell_2 y_2'(0), \tag{29}$$

$$\ell_1^2 n_1 y_1''(1) = \ell_2^2 n_2 y_2''(0)$$

where $\ell_i = L/L_i$; and $n_i = (EI)_i/(EI)$. The characteristic equations (19 and 22) of the uncracked and the corresponding cracked L-frames are:

$$g_1(\beta) = \begin{vmatrix} \underset{\sim}{U}_1(A) & \underset{\sim}{0} \\ \underset{\sim}{U}_2(B) & \underset{\sim}{U}_5(B) \\ \underset{\sim}{0} & \underset{\sim}{U}_6(C) \end{vmatrix} = 0 \tag{19b}$$

$$g_2(\bar{\beta}) = \begin{vmatrix} \underset{\sim}{U}_1(A) & \underset{\sim}{0} & \underset{\sim}{0} \\ \underset{\sim}{U}_3(e) & \underset{\sim}{U}_4(e) & \underset{\sim}{0} \\ \underset{\sim}{0} & \underset{\sim}{U}_2(B) & \underset{\sim}{U}_5(B) \\ \underset{\sim}{0} & \underset{\sim}{0} & \underset{\sim}{U}_6(C) \end{vmatrix} = 0 \tag{22b}$$

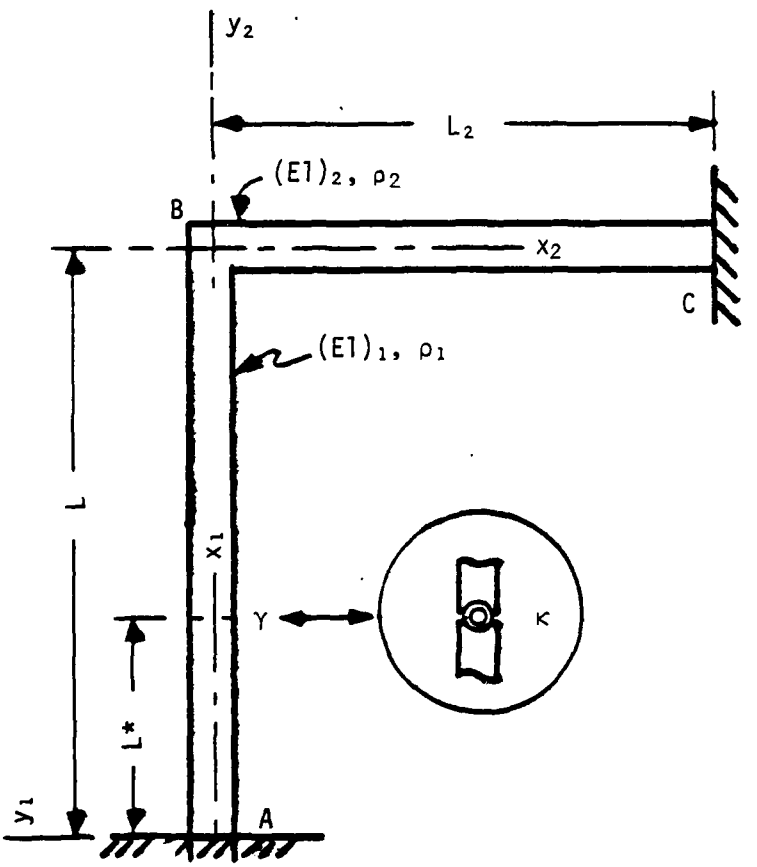

Figure 10. L-Frame with a single cracked section.

where β and $\bar{\beta}$ are the characteristic values of the uncracked and the corresponding cracked L-frames, such that $\beta^4 = \omega^2\rho L^4/(EI)$ as referred to the reference beam, the vertical leg. $\underset{\sim}{U}_1(A)$ and $\underset{\sim}{U}_6(C)$ are (2 x 4) matrices, related to the anchor conditions at A and C; specifically for fixed ends as shown in Figure 10, $\underset{\sim}{U}_1(A)$ has thus the same expression as (25), $\underset{\sim}{U}_6(C)$ differs from (26) since the end conditions are different, that is

$$\underset{\sim}{U}_1(A) = \begin{bmatrix} 1 & 0 & 1 & 0 \\ 0 & 1 & 0 & 1 \end{bmatrix} \tag{29}$$

$$\underset{\sim}{U}_6(C) = \begin{bmatrix} \cosh(\alpha_2\beta) & \sinh(\alpha_2\beta) & \cos(\alpha_2\beta) & \sin(\alpha_2\beta) \\ \sinh(\alpha_2\beta) & \cosh(\alpha_2\beta) & -\sin(\alpha_2\beta) & \cos(\alpha_2\beta) \end{bmatrix} \tag{30}$$

where $\alpha_i = \beta_i/\beta$. $\underset{\sim}{U}_2(B)$ and $\underset{\sim}{U}_5(B)$ are (4 x 4) matrices resulting from the continuity conditions and constraints at the corner (2^a), that

$$\underset{\sim}{U}_2(B) = \begin{bmatrix} \underset{\sim}{U}_7(\beta;1,1) \\ \underset{\sim}{U}_8(\beta;1,1) \\ \underset{\sim}{0} \end{bmatrix} \text{ and } \underset{\sim}{U}_5(B) = \begin{bmatrix} -\underset{\sim}{U}_7(\beta;0.2) \\ \underset{\sim}{0} \\ \underset{\sim}{U}_8(\beta;0,2) \end{bmatrix}$$

where

$$\underset{\sim}{U}_7(\beta;\xi,i) = \begin{bmatrix} \alpha_i \ell_i[\sinh(\alpha_i\beta\xi) & \cosh(\alpha_i\beta\xi) & -\sin(\alpha_i\beta\xi) & \cos(\alpha_2\beta\xi) \\ n_i\alpha_i^2 e_i^2[\cosh(\alpha_i\beta\xi) & \sinh(\alpha_i\beta\xi) & -\cos(\alpha_i\beta\xi) & -\sin(\alpha_1\beta\xi)] \end{bmatrix} \tag{31}$$

and

$$\underset{\sim}{U}_8(\beta;\xi,i) = [\cosh(\alpha_i\beta\xi) \quad \sinh(\alpha_i\beta\xi) \quad \cos(\alpha_i\beta\xi) \quad \sin(\alpha_i\beta\xi)] \tag{32}$$

where $n_i = (EI)_i/(EI)$ and $\ell_i = L/L_i$. $\underset{\sim}{U}_3(e)$ and $\underset{\sim}{U}_4(e)$ are unchanged as in the simple beam, (27, 28). The solutions of equations (19b, 22b) are substituted into (20) to solve for the modal frequencies of the uncracked and the corresponding cracked L-frames, $\{\omega_i\}$ and $\{\omega_i - \Delta\omega_i\}$ respectively. Figure 11 illustrates the measurements of $R_1 = 0.0363$ and $R_2 = 0.031$ for an L-frame with $\ell_2 = 1.333$, $n_2 = 1$, and $\alpha_2 = 0.75$, using the vertical leg as the reference member, and a slenderness ratio of 0.05. The solutions of e are multivalued at .140, .155, .480, and .530. If $R_3 = 0.0109$ is also available, the pair of damage characteristics are then determined at $\gamma = a/b = 0.4$ and $e = .480$. It is noted that the function $g_2(\bar{\beta})$ will be changed when the cracked section is in the horizontal leg, instead of the vertical leg. The same expression as in (22b) results when the designations of the horizontal and vertical legs are reversed, resulting in a new $g_3(\beta^*) = 0$. In other words, the set of $\{\beta\}$ corresponds to (γ, e) on the vertical leg; and the set of $\{\beta^*\}$ corresponds to (γ^*, e^*) on the horizontal leg. A given measure of $\{R_i\}$, therefore, will be consistent with only one pair of the damage characteristics. Hence, the frequency change measurement determines the location (e) and the intensity (γ) of the damage uniquely in an L-frame.

The unique solution will not be available for a special case when the expressions of $g_2(\bar{\beta})$ and $g_3(\beta^*)$, duplicate. Such is the case for L-frame of equal legs. It is shown in Figure 12 that the given measurements $R_1 = 0.0363$, $R_2 = 0.0061$ and $R_3 = 0.046$ for an L-frame of slenderness ratio 0.05 identify the damage location $e = 0.05$ and the damage intensity $\gamma = 0.6$ in either one of the legs.

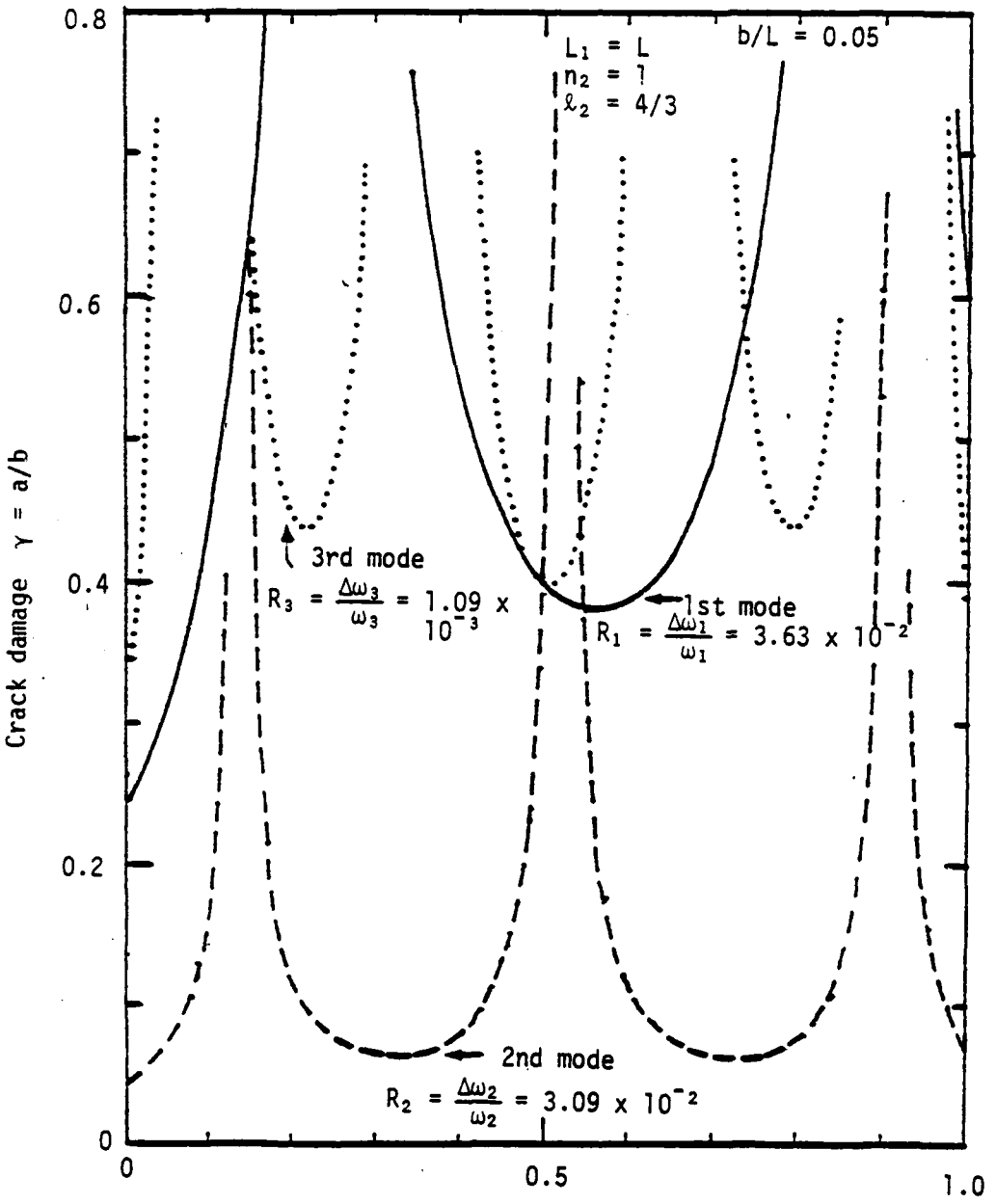

Figure 11. Damage diagnosis in L-Frame

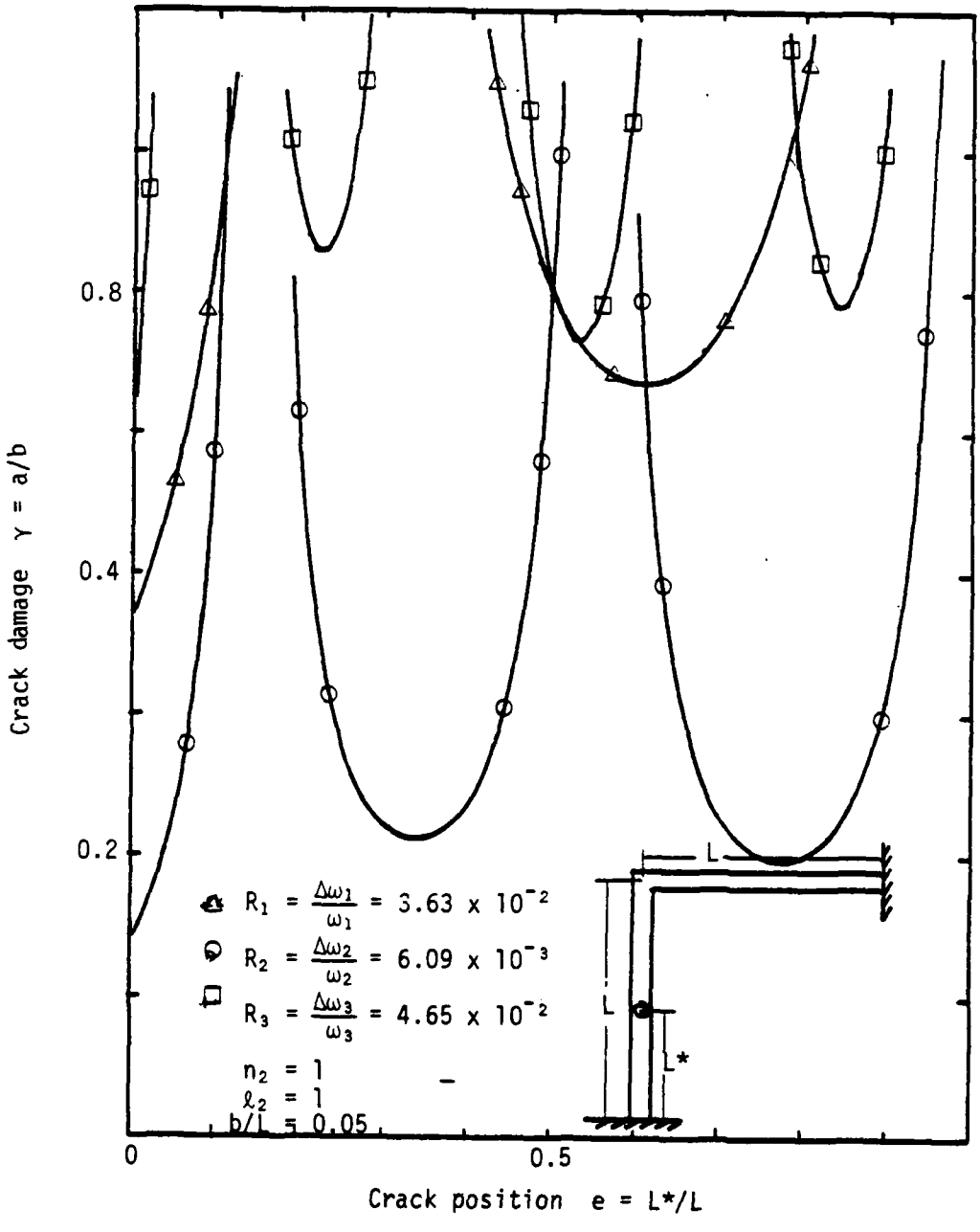

Figure 12. Damage diagnosis in equal leg L-frame.

3.3 U-Frame

The modal analysis of a U-frame is similar to that of an L-frame with an additional beam section. Figure 13 shows the geometry and possible crack location. In addition to the end conditions at two anchors, there are continuity conditions at the corners and the kinetic equation defining the motion of the horizontal beam which is not constrained in axial motion. The end conditions will be governed by how the ends C and D are anchored. The corner conditions are the continuity conditions and the geometrical constraint. At the corner A in the dimensionless expressions:

$$\ell_1 y_1'(1) = \ell_2 y_2'(0),\ n_1 \ell_1^2 y_1''(1) = n_2 \ell_2^2 y_2''(0),\ \text{and}\ y_2(0) = 0 \tag{33}$$

At the corner B:

$$\ell_2 y_2'(1) = \ell_3 y_3'(0),\ n_2 \ell_2^2 y_2''(1) = n_3 \ell_3^2 y_3''(0),\ \text{and}\ y_2(1) = 0. \tag{34}$$

The motions of the horizontal beam (AB) are

$$y_1(A) = -y_3(B) \quad \text{or} \quad y_1(1) = -y_3(0) \tag{35}$$

$$n_1 \ell_1^3 y_1'''(A) + n_3 \ell^3 y_3'''(B) = -\beta_2^4 n_2 \ell_2^3 y_1(A) \tag{36}$$

or

$$n_1 \ell_1^3 y_1'''(1) + \alpha_2^4 \beta^4 n_2 \ell_2^3 y_1(1) + n_3 \ell_3^3 y_3'''(0) = 0$$

where $\ell_i = L/L_i$, $n_i = (EI)_i/(EI)$ and $\beta_2^4 = \omega^2 p_2 L_2^4/(EI)_2$. The condition (35) is evident with reference to the coordinates shown

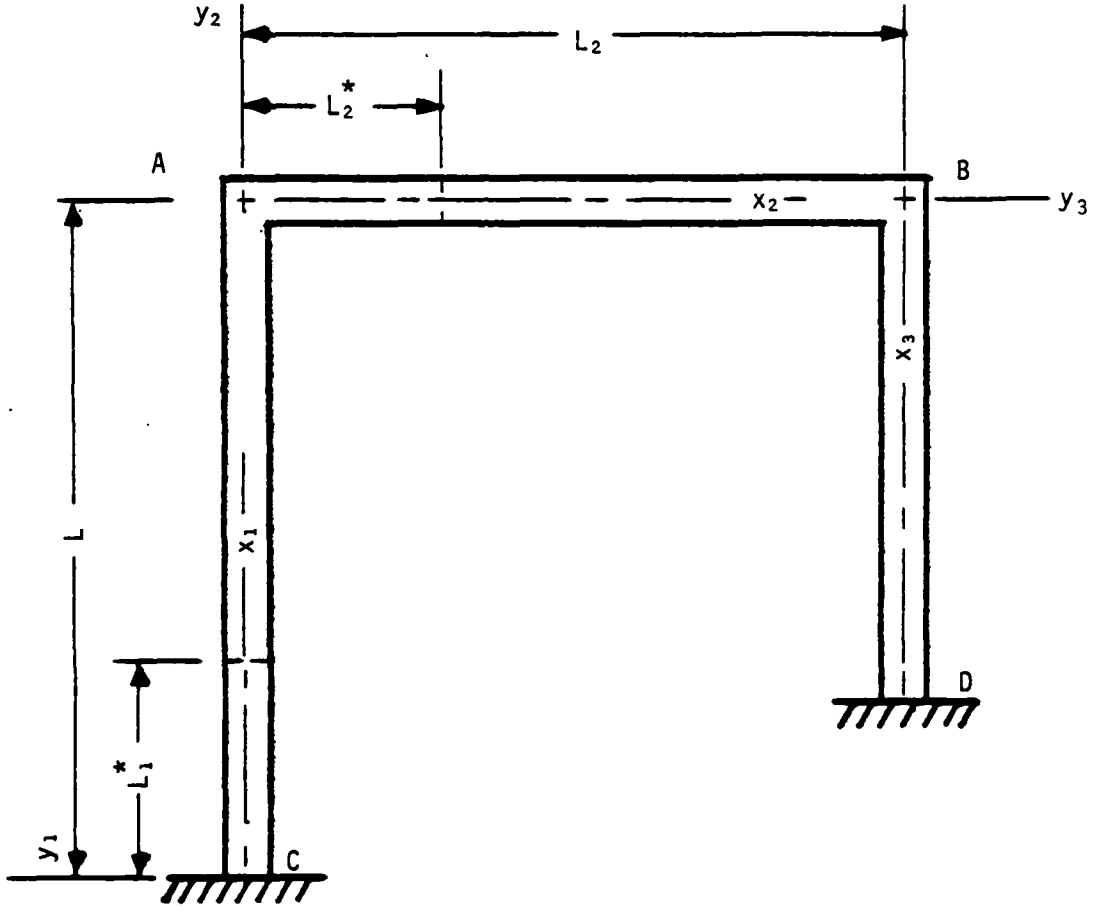

Figure 13. U-Frame with cracked section.

in Figure 13. To arrive at (36), we shall refer to Figure 14 for cross shears, which are the axial driving forces for the horizontal beam (AB). The axial acceleration of the horizontal beam shall be the same as the lateral acceleration of the vertical leg at either of the corners A and B; that is,

$$V_1(L) + V_3(0) = (\rho_2 L_2)[-\ddot{y}_1(L)].$$

At modal oscillation, $\ddot{y}_1(L) = -\omega^2 y_1(L)$. Hence for $V = -EIy'''$,

$$-(EI)_1 y_1'''(L) - (EI)_3 y_3'''(0) = \rho_2 L_2 \omega^2 y_1(L),$$

or

$$n_1 y_1'''(L) + n_3 y_3'''(0) + [\omega^2 \rho_2 L_2^4/(EI)_2][(EI)_2/EI] y_1(L) L_2^3 = 0$$

When expressed in dimensionless form, the expression in (36) results. For an uncracked U-frame, there are two pairs of end conditions for the two anchors, and eight corner conditions at A and B for the three sets of coefficients {A, B, C, D} of beam equation (18) and the characteristic parameter β. The resulting characteristic equation (19) for the uncracked U-frame is arranged as

$$g_1(\beta) = \begin{bmatrix} \underset{\sim}{U}_1(C) & \underset{\sim}{0} & \underset{\sim}{0} \\ \underset{\sim}{U}_2(A) & \underset{\sim}{U}_5(A) & \underset{\sim}{0} \\ \underset{\sim}{U}_6(A) & \underset{\sim}{U}_7(B) & \underset{\sim}{U}_8(B) \\ \underset{\sim}{0} & \underset{\sim}{0} & \underset{\sim}{U}_9(D) \end{bmatrix} = 0 \qquad (19c)$$

where all submatrices are referred to the positions on the U-frame for convenience of discussion. For instance, as C and D are the two ends of the U-frame, the matrices $\underset{\sim}{U}_1(C)$ and $\underset{\sim}{U}_9(D)$

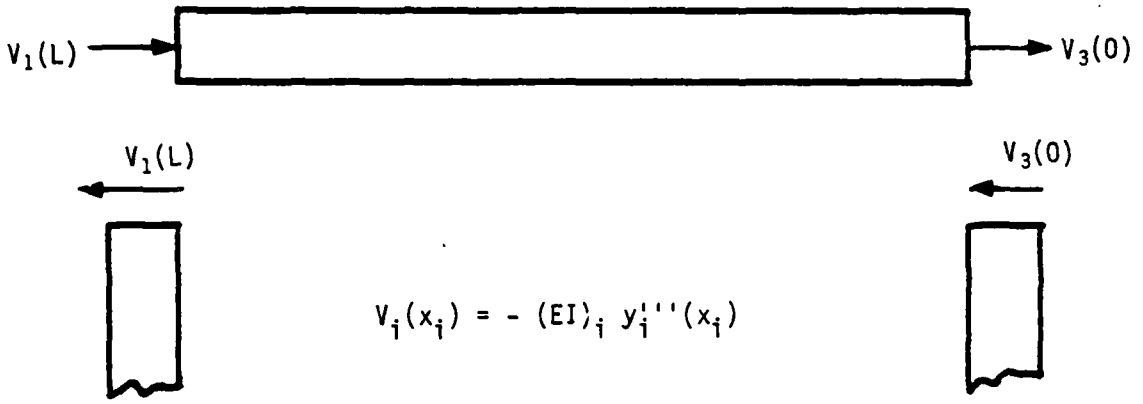

Figure 14. Cross-shears in the vertical legs.

thus define the anchor conditions of the frame. For fixed endsas shown in Figure 13

$$\underset{\sim}{U}_1(C) = \begin{bmatrix} 1 & 0 & 1 & 0 \\ 0 & 1 & 0 & 1 \end{bmatrix}$$

$$\underset{\sim}{U}_9(D) = \begin{bmatrix} \cosh(\alpha_3\beta) & \sinh(\alpha_3\beta) & \cos(\alpha_3\beta) & \sin(\alpha_3\beta) \\ \sinh(\alpha_3\beta) & \cosh(\alpha_3 b) & -\sin(\alpha_3\beta) & \cos(\alpha_3\beta) \end{bmatrix}.$$

$\underset{\sim}{U}_2(A)$ and $\underset{\sim}{U}_5(A)$ are both (3 x 4) matrices which result from the continuity conditions at A, (33), that,

$$\underset{\sim}{U}_2(A) = \begin{bmatrix} \underset{\sim}{U}_{10}(\beta;1,1) \\ \\ \underset{\sim}{0} \end{bmatrix} \quad \text{and} \quad \underset{\sim}{U}_5(A) = \begin{bmatrix} -\underset{\sim}{U}_{10}(\beta;0,2) \\ \\ \underset{\sim}{U}_{11}(\beta;0,2) \end{bmatrix} \tag{37}$$

where

$$\underset{\sim}{U}_{10}(\beta;\xi,i) = \begin{bmatrix} \alpha_i \ell_i[\sinh(\alpha_i\beta\xi) & \cosh(\alpha_i\beta\xi) & -\sin(\alpha_i\beta\xi) & \cos(\alpha_i\beta\xi)] \\ n_i \alpha_i^2 \ell_i^2[\cosh(\alpha_i\beta\xi) & \sinh(\alpha_i\beta\xi) & -\cos(\alpha_i\beta\xi) & -\sin(\alpha_i\beta\xi)] \end{bmatrix} \tag{38}$$

and

$$\underset{\sim}{U}_{11}(\beta;\xi,i) = [\cosh(\alpha_i\beta\xi) \quad \sinh(\alpha_i\beta\xi) \quad \cos(\alpha_i\beta\xi) \quad \sin(\alpha_i\beta\xi)] \tag{39}$$

The matrices $\underset{\sim}{U}_6(A)$, $\underset{\sim}{U}_7(B)$ and $\underset{\sim}{U}_8(B)$ are all (5 x 4) as groupings of the corner conditions at B, (34), and the equations of motion of the horizontal beam (AB), (35, 36); they are

$$\underset{\sim}{U}_6(A) = \begin{bmatrix} \underset{\sim}{U}_{11}(\beta;1,1) \\ \underset{\sim}{U}_{12}(\beta;1,1) + \alpha_2^4 \beta n_2 \ell_2^3 \, \underset{\sim}{U}_{11}(\beta;1,1) \\ \underset{\sim}{0} \end{bmatrix} \tag{40}$$

$$\underset{\sim}{U}_7(\beta) = \begin{bmatrix} \underset{\sim}{0} \\ \underset{\sim}{U}_{10}(\beta;1,2) \\ \underset{\sim}{U}_{11}(\beta;1,2) \end{bmatrix} \tag{41}$$

and

$$\underset{\sim}{U}_8(\beta) = \begin{bmatrix} \underset{\sim}{U}_{11}(\beta;0,3) \\ \underset{\sim}{U}_{12}(\beta;0,3) \\ -\underset{\sim}{U}_{10}(\beta;0,3) \\ \underset{\sim}{0} \end{bmatrix} \tag{42}$$

where

$$\underset{\sim}{U}_{12}(\beta;\xi,i) = n_i \ell_i^3 \alpha_i^3 \left[\sinh(\alpha_i\beta\xi)\cosh(\alpha_i\beta\xi)\sin(\alpha_i\beta\xi) - \cos(\alpha_i\beta\xi)\right] \tag{43}$$

Depending on the choice of the reference member in the frame, the geometry/material ratios can be simplified. For instance, if the horizontal member is chosen as the reference, $\alpha_2 = \ell_2 = n_2 = 1$ and $\beta_2 = \beta$. The characteristic equation, $g_2(\bar{\beta}) = 0$, is obtained after expanding the determinant (19c) by an order of 4, with the introduction of the fracture hinge conditions (21), or the submatrices $\underset{\sim}{U}_3(e)$ and $\underset{\sim}{U}_4(e)$, (27, 28). For the case when the crack occurs on the vertical leg, AC, we have

$$g_2(\bar{\beta}) = \begin{vmatrix} \underset{\sim}{U}_1(C) & \underset{\sim}{0} & \underset{\sim}{0} & \underset{\sim}{0} \\ \underset{\sim}{U}_3(e) & \underset{\sim}{U}_4(e) & \underset{\sim}{0} & \underset{\sim}{0} \\ \underset{\sim}{0} & \underset{\sim}{U}_2(A) & \underset{\sim}{U}_5(A) & \underset{\sim}{0} \\ \underset{\sim}{0} & \underset{\sim}{U}_6(A) & \underset{\sim}{U}_7(B) & \underset{\sim}{U}_8(B) \\ \underset{\sim}{0} & \underset{\sim}{0} & \underset{\sim}{0} & \underset{\sim}{U}_9(D) \end{vmatrix} = 0$$

When the crack occurs on the horizontal member, AB, the hinge is between A and B, resulting in:

$$g_2(\bar{\beta}) = \begin{matrix} \underset{\sim}{U}_1(C) & \underset{\sim}{0} & \underset{\sim}{0} & \underset{\sim}{0} \\ \underset{\sim}{U}_2(A) & \underset{\sim}{U}_5(A) & \underset{\sim}{0} & \underset{\sim}{0} \\ \underset{\sim}{0} & \underset{\sim}{U}_3(e) & \underset{\sim}{U}_4(e) & \underset{\sim}{0} \\ \underset{\sim}{U}_6(A) & \underset{\sim}{0} & \underset{\sim}{U}_7(B) & \underset{\sim}{U}_8(B) \\ \underset{\sim}{0} & \underset{\sim}{0} & \underset{\sim}{0} & \underset{\sim}{U}_9(D) \end{matrix} = 0 \qquad (22d)$$

Notice that the fracture hinge matrices (27, 28) are inserted where they separate the submatrices in a column which are defined at the two end points of the cracked member. To obtain the characteristic equation, when a crack is in the other vertical leg, one may either insert the fracture hinge matrices separating $\underset{\sim}{U}_8(B)$ and $\underset{\sim}{U}_9(D)$, or use the similar expression of (22c) with a left/right transfer of the configuration. In the expressions (22c) and (22d), the sensitivity number I is defined as

$$\theta = [EI/\kappa L]_i \qquad (44)$$

where the index 'i' denotes the specific cracked member in the structure.

The characteristic equations (19c, 22c, and 22d) are quite complex. The solutions of (θ, e) then (γ, e) = $G(R_i)$, equation (4), are thus programmed in a computer without curve plots such as those in the simple beams (Figures 7 through 9) and the L-frames (Figures 11, 12). Both characteristic equations, (22c and 22d) are used in the diagnosis. Again three measurements of frequency variation, R_1, R_2, and R_3, are sufficient for the determination of the fracture characteristics of a single crack. Except, of course, a U-frame with equal vertical legs, which are anchored the same way, will have symmetrical crack locations and damage intensities that are not differentiable. In the computer code, a crack is first sought on the vertical legs and then on

the horizontal member. In the deterministic case for a single crack, the three measurements of frequency variations will locate the crack specifically on the member of the U-frame where the crack occurs. However, when inadequate measurements are given, probable fracture locations may occur on both of the legs and the horizontal member. For instance, as indicated by equations (6, 7), we have two measurements of frequency variations,

$$\{R_1, R_2\} = \{0.022, 0.005\}$$

for a symmetrical U-frame. Referring to the horizontl member as the reference beam we have

$$n_2 = \ell_2 = \alpha_2 = 1,\ n_1 = n_3 = 1,\ \ell_1 = \ell_3 = 1.25,\ \alpha_1 = \alpha_3 = 0.8$$

The admissible solututions are

$$\{(\theta,e)\}_1 = \{(0.031, 0.050)\ (0.426, 0.390\}$$
$$\{(\theta,e)\}_2 = \{(0.095, 0.078)\ (0.180, 0.187)\ (0.180, 0.813)\ (0.095, 0.922)\}$$
$$\{(\theta,e)\}_3 = \{(0.426, 0.610)\ (0.031, 0.950\}$$

Because of the symmetry condition, there are only four pairs of solutions. They are

$$\{(\theta,e)\}_1 = \{(0.031, 0.050)\ (0.426, 0.390)\}$$
$$\{(\theta,e)\}_2 = \{0.095, 0.078)\ \ (0.180, 0.187)\}$$

as shown in Figure 15. With reference to equations (6, 7), it is proposed that the crack occurs at the most likely location, e, where the largest probability function, p_j, occurs. It is assumed that the largest p_j of the set in turn corresponds to the location, e, where the moment distribution has its greatest

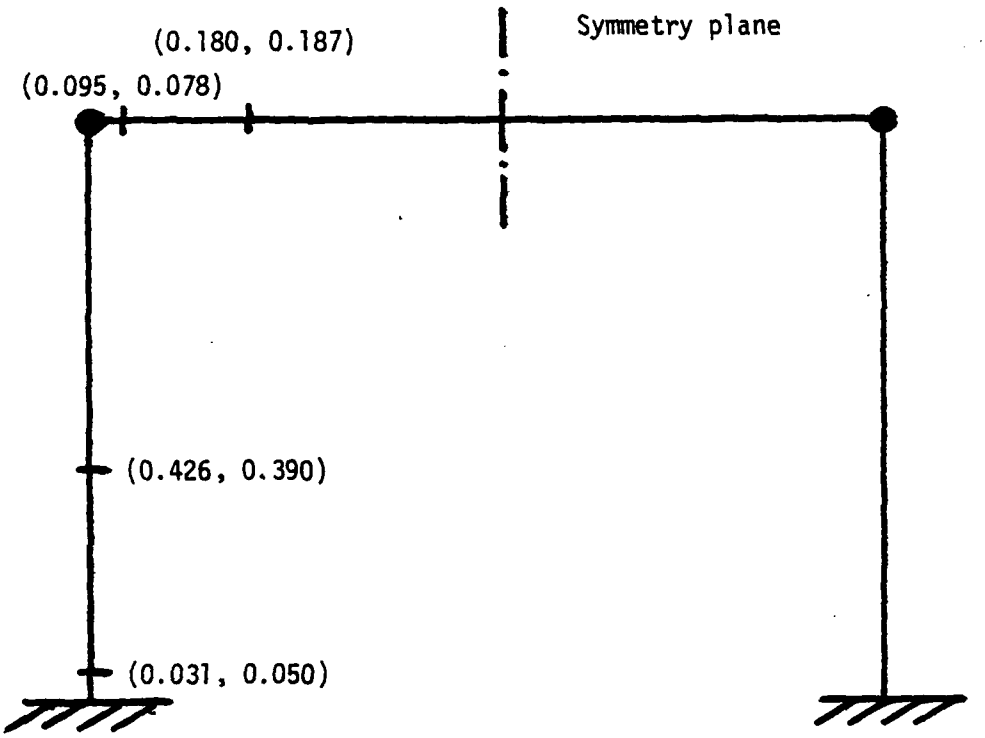

$R_1 = 0.022 \quad R_2 = .005$

Figure 15. Fracture damage characteristic pair (θ,e)

value among the possible solutions. Figures 16 and 17 illustrate the modal shapes and the corresponding moment distributions of the symmetrical U-frame. For illustrative purposes we may assume that

$$p_j \doteq m_j = |M(e_j)| \Big/ \sum_j |M(e_j)|$$

The approximation indicates that in the present example, since R_1 is more than four times R_2, the resisting moment $M(e_j)$ is to be based only on the first mode moment distribution. Hence

$$\{p_j\} = \{m_j\} = \{0.45 \quad 0.15 \quad 0.17 \quad 0.23\}$$

The most probable location is therefore on either of the vertical legs at a distance of 0.05 L_1 from the anchor. The fracture damage intensity, γ, corresponding to the sensitivity number, $\theta = 0.031$, depends on the slenderness ratio (b/L), *re: equation* (23). If we use a rectangular cross section, for a 5 percent slenderness ratio, the damage intensity is $\gamma = 0.33$; for a 1.5 percent slenderness ratio, it takes a damage intensity of $\gamma = 0.52$ to effect a corresponding frequency change. The values of γ can be approximately deduced by referring to Figure 5.

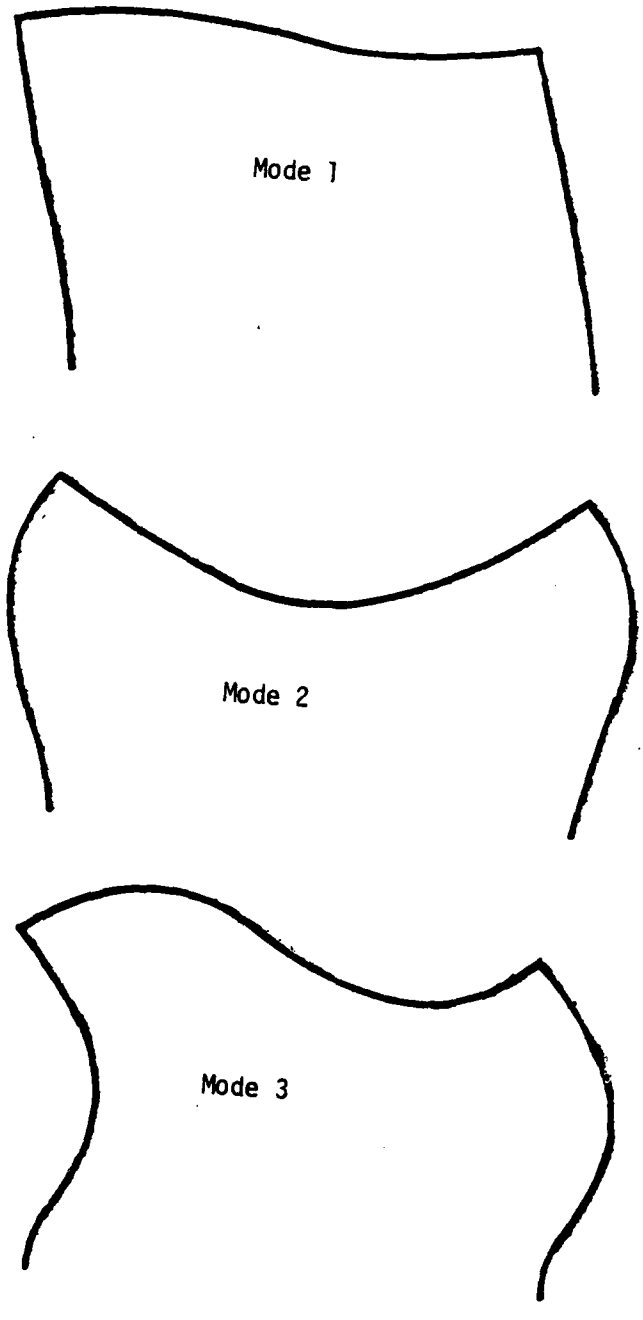

Figure 16. Modal shape of a symmetrical U-frame.
$\ell_1 = \ell_3 = 1.25$, $n_1 = n_3 = 1$, $\alpha_1 = \alpha_3 = 0.8$

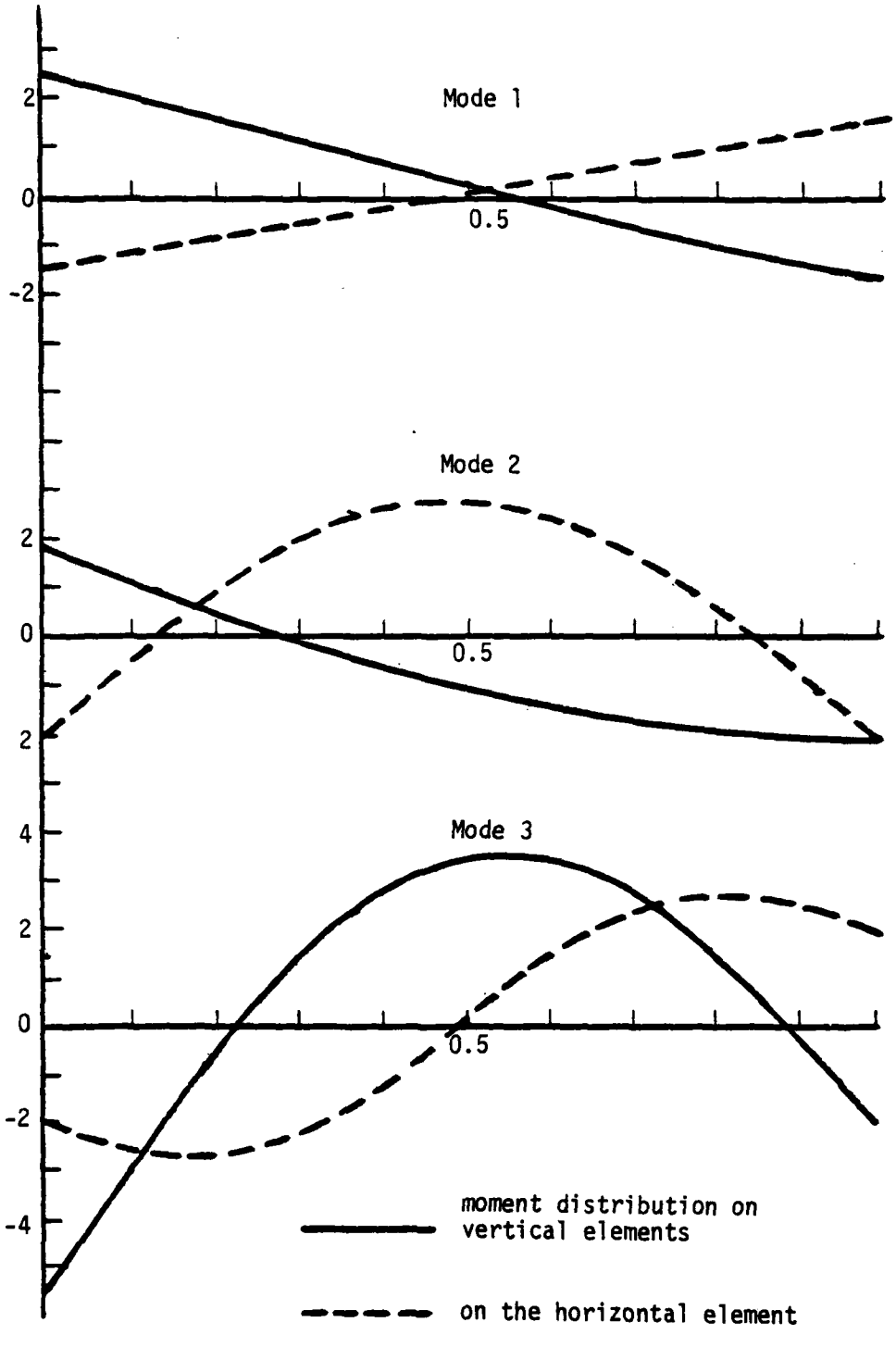

Figure 17. Moment distributions at modal oscillation in a symmetrical U-frame.

$\ell_1 = \ell_3 = 1.25$, $n_1 = n_3 = 1$, $\alpha_1 = \alpha_3 = 0.8$

4.0 CONCLUSION

The present report addresses the effect of fracture damage on the stiffness, then on the modal frequencies of a structure. The intensity of damage and its location, (γ, e), can be identified if sufficient measurements of frequency variations, $\{R_i\}$, and the damage function, $G_R(R_i)$, can be established. For simple structures such as uniform beams, L-frames and U-frames, the analytical form of the damage function can be readily established or programmed in computers. The deterministic solution depends on the adequate number of measurements in frequency variations. When an insufficient number of measurements is available, the diagnosis can still be carried out on a probabilistic base. At present, however, there is no quantitative measure of probability, since the postulation of using moment distribution as an analogy to the probability distribution is at best qualitative.

The introduction of the fracture hinge indeed simplifies the mathematics of damage function. The assumptions and the subsequent development are based on the concept that the strain energy increment under constant load comes from the total conversion from the surface energy that results from creation of the crack surface. The very simplicity is the beauty of the theory. The extent of deviation from the physical behavior of the structure must yet be established by experiment. Further work may then be expanded to cracks of different geometry.

It is noticed that, while the fracture damage is characterized by the pair (γ, e), $\gamma = a/b$ and $e = L^*/L$, the damage intensity is really measured by the sensitivity number, θ. Indeed, the greater is the fracture damage intensity, the greater is the sensitivity number; but for a given γ, the more slender the beam, the smaller is θ. From a practical point of view, the sensitivity number is indicative of how easy or difficult it is to detect

a crack. A very slender beam may have a severe crack on it (i.e., γ large), yet changes in the modal frequencies would be small, thus difficult to detect.

In a fractured structure, the modal frequency variations are, of course, influenced by the location of the crack, $e = L^*/L$. The sensitivity measure should seem to be a number combining both θ and e. However, the fracture hinge matrices $\underset{\sim}{U}_3(\bar{\beta}; e, \theta)$ and $\underset{\sim}{U}_4(\bar{\beta}; e)$, equations (27, 28) in the frequency equation (22), demonstrate that the two quantities must be treated as two separate entities. It is this very property that allows determination of both the location and intensity of the fracture damage.

REFERENCES

1. Liebowitz, H., "Fracture and Carrying Capacity of Notched Columns," Chap. 4, Fracture, Vol. IV, ed., Liebowitz, Acad. Press, 1969, pp. 113-171.

2. Bennett, J. G., Ju, F. D., and Anderson, C. A., "An Investigation of Failure Mechanisms for HTGR (High Temperature Gas-cooled Reactor) Core Supports," LASL Report LA-NUREG-6639-MS (Dec. 1976).

3. Ju, F. D., Bennett, J. G., and Anderson, C. A., "Structural Safety Analysis of HTGR Core Supports," Advances in Civil Engineering through Engineering Mechanics, Proc. 2nd EMD Specialty Conference, ASCE, 1977, pp. 427-430.

4. ASME B and PV Code, Sec. XI, ART. IWA-2000, 1974.

5. Chondros, I. G., and Dimarogonas, A. D., "Identification of Cracks in Welded Joints of Complex Structures," Jour. Sound Vibra., 1980, pp. 531-538.

6. Tada, H., Paris, P., and Irwin, G., "Compliance Calibration Methods," The Stress Analysis of Cracks Handbook, Del Res. Corp., 1973, pp. 1.10-1.12.

7. Bentham, J. P., and Koiter, W. T., "Asymptotic Approximation to Crack Problems," Methods of Analysis and Solutions of Crack Problems, Mechanics of Fracture I, ed., G. C. Sih, 1973, pp. 155-158.

8. Young, D., and Felgar, R. P., Jr., Tables of Characteristic Functions Representing Normal Modes of Vibration of a Beam, Eng. Res. Bul. No. 4913, BER, University of Texas, July 1949.

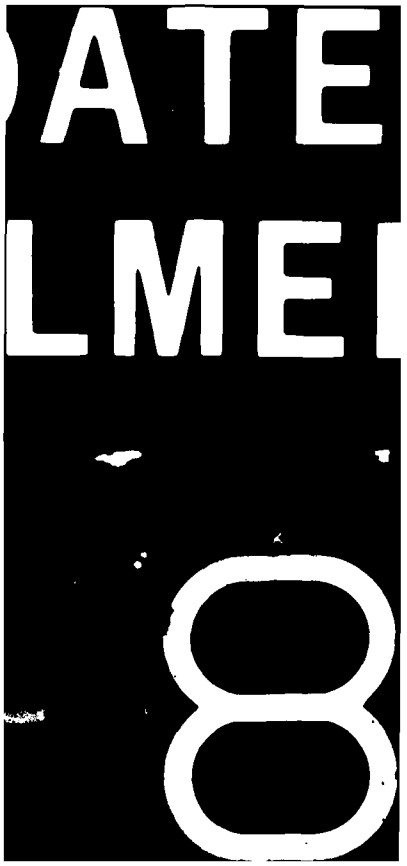
ATE
LME
8